ARTICLE IN PRESS

Available online at www.sciencedirect.com

ScienceDirect

Advances in Space Research xxx (2019) xxx–xxx

ADVANCES IN SPACE RESEARCH (a COSPAR publication)

www.elsevier.com/locate/asr

Hard X-ray cataclysmic variables

D. de Martino [a,*], F. Bernardini [b,a,c], K. Mukai [d,e], M. Falanga [f,g], N. Masetti [h,i]

[a] Istituto Nazionale di Astrofisica, Osservatorio Astronomico di Capodimonte, Salita Moiariello 16, I-80131 Napoli, Italy
[b] Istituto Nazionale di Astrofisica, Osservatorio Astronomico di Roma, Via Frascati 33, I-00040 Monte Porzio Catone, RM, Italy
[c] New York University Abu Dhabi, Saadiyat Island, Abu Dhabi 129188, United Arab Emirates
[d] CRESST and X-ray Astrophysics Laboratory, NASA Goddard Space Flight Center, Greenbelt, MD 20771, USA
[e] Department of Physics, University of Maryland, Baltimore County, 1000 Hilltop Circle, Baltimore, MD 21250, USA
[f] International Space Science Institute (ISSI), Hallerstrasse 6, CH-3012 Bern, Switzerland
[g] International Space Science Institute Beijing, No. 1 Nanertiao, Zhongguancun, Haidian District, 100190 Beijing, China
[h] Istituto Nazionale di Astrofisica, Osservatorio di Astrofisica e Scienza dello Spazio di Bologna, Via Gobetti 93/3, I-40129 Bologna, Italy
[i] Departamento de Ciencias Físicas, Universidad Andrés Bello, Fernández Concha 700, Las Condes, Santiago, Chile

Received 5 June 2019; received in revised form 2 September 2019; accepted 3 September 2019

Abstract

Among hard X-ray Galactic sources detected with the *Swift* and *INTEGRAL* surveys, those discovered as accreting white dwarf binaries have surprisingly boosted in number in the recent years. The majority are identified as magnetic Cataclysmic Variables of the Intermediate Polar type, suggesting this subclass as an important constituent of the Galactic population of X-ray sources. We here review and discuss the X-ray emission properties of newly discovered sources in the framework of an identification programme with the *XMM-Newton* satellite that increased the sample of this subclass by a factor of two.

Keywords: X-Rays: binaries; Stars: cataclysmic variables; Accretion; Accretion discs

1. Introduction

Cataclysmic Variables (CVs) are low-mass close binary systems composed by a white dwarf (WD) primary accreting material lost from a Roche-lobe filling, late-type companion star. According to the variety of observed phenomenology they are grouped in several subclasses (see review Warner, 1995). Two main categories can be identified: the magnetic systems (mCVs) harbouring WD primaries with strong magnetic fields ($B_{WD} \geqslant 10^6$ G) and non-magnetic CVs. The magnetic systems are also subdivided in two groups, the polars that contain highly ($B_{WD} \sim 14 - 230 \times 10^6$ G) magnetised WDs, and the intermediate polars (IPs) believed to harbour low magnetic field primaries ($B_{WD} \lesssim 10^7$ G) (see reviews by Cropper, 1990; Ferrario et al., 2015; Mukai, 2017). In both subclasses the WD magnetic field plays a key role in shaping the accretion flow. In the polars the B-field is strong enough to lock, or quasi-lock, the WD rotation at the binary orbit, and to channel matter from the donor star onto the WD polar caps through an accretion stream. Thus, polars show strong periodic orbital variability at all wavelengths (e.g. Schwope et al., 1998). In IPs, instead, the weaker field is not able to synchronise the WD rotation at the binary orbit allowing fast spin rates ($P_{spin=\omega} \ll P_{orb=\Omega} \sim$ hrs) and the formation of an accretion disc truncated at the magnetospheric boundary where the magnetic pressure balances

* Corresponding author.
E-mail addresses: domitilla.demartino@inaf.it (D. de Martino), federico.bernardini@inaf.it (F. Bernardini), Koji.Mukai@nasa.gov (K. Mukai), mfalanga@issibern.ch (M. Falanga), nicola.masetti@inaf.it (N. Masetti).

https://doi.org/10.1016/j.asr.2019.09.006
0273-1177/

the ram pressure. Depending on system parameters, such as orbital period, magnetic field strength and mass accretion rate, IPs may accrete via a disc (disc-fed systems), without a disc (disc-less) or in a hybrid mode in the form of disc overflow, which can be diagnosed through the presence of spin, orbital and sidebands periodicities at different wavelengths (Hellier, 1995; Norton et al., 1996, 1997).

The accretion flow close to the WD surface is channeled along the magnetic field lines, reaching supersonic velocities and producing a stand-off shock above the WD surface (Aizu, 1973). The post-shock region (PSR) is hot ($kT \sim 10$–50 keV) and cools via thermal Bremsstrahlung (hard X-rays) and cyclotron radiation, emerging in the optical/nIR band. Both emissions are partially thermalized by the WD surface and re-emitted in the soft X-rays and/or EUV/UV domains. The relative proportion of the two cooling mechanisms strongly depends on the B-field strength and local mass accretion rate. Cyclotron radiation dominates in the high field polars and is efficient in suppressing high PSR temperatures (Woelk and Beuermann, 1996; Fischer and Beuermann, 2001). An optically thick soft X-ray ($kT_{bb} \sim 30$–50 eV) emission due to reprocessing (van Teeseling et al., 1994) or to heating due to blobby accretion (Woelk and Beuermann, 1992) was also found to be strong in polars, explaining why they where found numerous in previous soft X-ray surveys (e.g. *ROSAT*), largely outnumbering IPs (Beuermann, 1999; Schwope et al., 2002). The PSR has been diagnosed in details through circular and linear polarimetry and spectro-polarimetry at optical/nIR wavelengths, in the polars only, revealing complex field topology with differences between the primary and secondary poles (e.g. Potter et al., 2004; Beuermann et al., 2007; Ferrario et al., 2015). In some cases differences in the magnetic field strengths have also been found between the PSR region and the WD photosphere, the latter inferred from Zeeman splitting of hydrogen lines (e.g. Schwope et al., 1995; Ferrario et al., 2015). On the contrary, most IPs do not show optical/nIR polarization, with only 11 systems found to be polarised at a few percent (see Ferrario et al., 2015; Potter and Buckley, 2018). Their magnetic field strengths are consequently difficult to measure and are loosely estimated in the range ~ 5–30×10^6 G. These polarised IPs are all found at long orbital periods, above the 2–3 h orbital period gap, and could represent the long-sought progenitors of low-field polars that will evolve into synchronism.

The complex geometry and emission properties of mCVs make these low-mass X-ray binaries ideal laboratories to study in details accretion processes in moderate magnetic field environments, but also help in understanding the role of magnetic fields in close-binary evolution. Indeed, the incidence of magnetism among CVs is $\sim 25\%$, compared to $\sim 6-10\%$ of isolated magnetic WDs (Ferrario et al., 2015). This would either imply CV formation is favoured by magnetism or CV production enhances magnetism (Tout et al., 2008). In addition, mCVs are the brightest X-ray emitting CVs, with X-ray luminosities ranging from a few $\sim 10^{30}$ erg s^{-1} to $\sim 10^{34}$ erg s^{-1}, and may play a crucial role in understanding Galactic X-ray binary populations.

We here review the recent progresses on mCVs obtained in the framework of an identification programme with the *XMM-Newton* mission, aiming at classifying new mCV candidates discovered in the hard X-ray surveys conducted by the *Swift* and *INTEGRAL* satellites. In Section 2 we report on the outcomes from these surveys. In Section 3 we summarize the new identifications, their temporal and spectral properties and in Section 4 the role of fundamental parameters. In Section 5 we conclude on the perspectives with future missions foreseen in the 2020–2030 timeframe.

2. Cataclysmic Variables in hard X-ray surveys

Our view of the hard X-ray sky dramatically changed thanks to the deep *INTEGRAL*/IBIS-ISGRI (Bird et al., 2016) and *Swift*/BAT (Oh et al., 2018) surveys with more than 1600 sources detected above 20 keV. These surveys have shown that our knowledge of the X-ray binary populations in the Galaxy was poor, surprisingly detecting a large number of accreting WD binaries, amounting to $\sim 25\%$ of the Galactic sources. Both the *INTEGRAL*/IBIS-ISGRI Galactic plane survey (Barlow et al., 2006; Krivonos et al., 2012; Bird et al., 2016) and the *Swift*/*BAT* survey (Oh et al., 2018), mainly covering high Galactic latitudes, reveal a high incidence of mCVs with $\sim 70\%$ of them belonging to the IP group. In Fig. 1 we show the accreting WD binaries detected from both surveys, comprising of a handful of previously known non-magnetic Dwarf Novae (DNs), old Novae and Symbiotics, many Nova-like systems (NLs) (most are still disputed to be magnetic), and the magnetic IPs and polars. This finding indicates that the subclass of IP-type mCVs is not as small as previously believed, suggesting them as potential important contributors to the Galactic X-ray source population. Indeed, the deep surveys of the Galactic centre conducted with *Chandra* (Muno et al., 2004), *XMM-Newton* (Heard and Warwick, 2013) and recently with *NuSTAR*, that overcomes the selection bias towards high temperatures of the *INTEGRAL*/IBIS-ISGRI and *Swift*/BAT surveys, (Perez et al., 2015; Hailey et al., 2016; Hong et al., 2016) all suggest the dominance of mCVs of the IP-type above $\sim 10^{31}$ erg s^{-1}. Whether these mCVs also dominate the Galactic ridge emission (GRXE) is still disputed based on *RXTE* (Revnivtsev et al., 2006), *Chandra* (Revnivtsev et al., 2009), *XMM-Newton* (Warwick et al., 2014) and *Suzaku* (Xu et al., 2016; Nobukawa et al., 2016) observations.

The negligible absorption in the hard X-rays makes these surveys unique for population studies. In particular the *Swift*/BAT survey, with a more uniform exposure over the sky was used to estimate the mCV space densities but with large uncertainties (Pretorius et al., 2013; Reis et al.,

Please cite this article as: D. de Martino, F. Bernardini, K. Mukai et al., Hard X-ray cataclysmic variables, Advances in Space Research, https://doi.org/10.1016/j.asr.2019.09.006

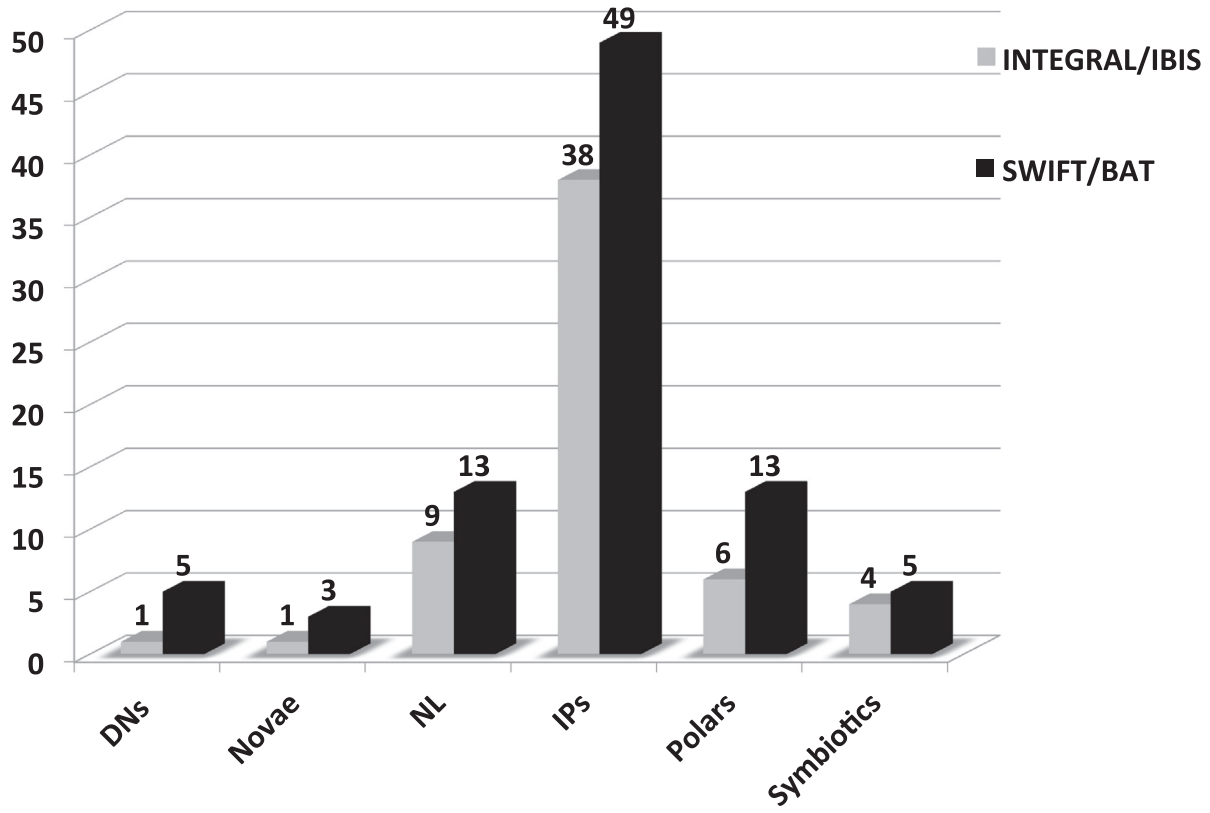

Fig. 1. The distribution of CV types detected by INTEGRAL/IBIS-ISGRI and Swift/BAT using the latest catalogue releases (misidentifications were corrected).

2013; Pretorius and Mukai, 2014) The *Gaia* DR2 release now offers the opportunity to assess the true space densities. Using the shallow flux-limits of the 70-month*Swift*/BAT sample of Pretorius and Mukai (2014) and the *Gaia* DR2 parallaxes, the IP space density results to be lower than previously estimated, with an upper limit of $< 1.3 \times 10^{-7}\,\mathrm{pc}^{-3}$ (Schwope, 2018). However, confirmation of this result needs larger samples from more sensitive surveys, such as that foreseen with the *eROSITA* satellite. Nevertheless, the recent release of the 105-month (Oh et al., 2018) and the parallel 100-month (Cusumano et al., 2014) *Swift*/BAT catalogues, reaching flux levels down to $\sim 7.2(\sim 5.4)$ and $8.4 \times 10^{-12}\mathrm{erg\,cm^{-2}\,s^{-1}}$ over 50 and 90% of the sky, respectively, are providing the opportunity to enlarge the sample of hard X-ray detected CVs and in particular of mCVs. For the current sample of hard X-ray mCVs, encompassing 50 confirmed IPs (see Table 1) and 13 polars, we obtained distances from the *Gaia* DR2 release using a distance prior based on the Galaxy model described in Bailer-Jones et al. (2018). [1] The majority are accurate with relative uncertainties less than 10%, restricting the sample to $\lesssim 1.8\,\mathrm{kpc}$ and $\lesssim 500\,\mathrm{pc}$ for 36 IPs and for the 13 polars, respectively. The derived distribution of hard X-ray luminosities in the *Swift*/BAT 14–195 keV band is shown in Fig. 2 for this sample of mCVs. It peaks at $L_{\mathrm{hard}} \sim 1.3 \times 10^{33}\,\mathrm{erg\,s^{-1}}$, but also extends to low luminosities ($\lesssim 10^{32}\,\mathrm{erg\,s^{-1}}$) where four systems are found, hinting to a bimodality. The presence of a putative still-hidden faint ($\sim 10^{31}\,\mathrm{erg\,s^{-1}}$) population of IPs was already envisaged by Pretorius and Mukai (2014) based on the 70-month *Swift*/BAT catalogue. These low-luminosity IPs should accrete at low rates and thus expected at short orbital periods (see also Section 3). Three of the four low-luminosity IPs have indeed $P_\Omega < 2\,\mathrm{h}$. The 13 confirmed hard X-ray polars detected so far (see Bernardini et al., 2014, 2017, 2019b; Gabdeev et al., 2017; Mukai, 2017) are found at $\lesssim 10^{33}\,\mathrm{erg\,s^{-1}}$, overlapping the low-luminosity IPs. Among them, those few with determined magnetic field strengths (up to $\sim 40 \times 10^6\,\mathrm{G}$), not be expected to be strong in hard X-rays, challenge our knowledge of the emission properties in mCVs. Whether the faint end of the mCV luminosity distribution is a mixture of the two classes or dominated by one of the two groups needs to be assessed by classifying still unidentified faint sources at the survey flux limits.

3. The increase of the mCV sample

Both BAT and IBIS-ISGRI catalogues, still carry tentative new CV identifications, with many sources claimed as magnetic, based on optical follow-ups (e.g. Masetti et al., 2012, 2013; Parisi et al., 2014; Thorstensen and Halpern,

[1] http://gaia.ari.uni-heidelberg.de/tap.html.

Please cite this article as: D. de Martino, F. Bernardini, K. Mukai et al., Hard X-ray cataclysmic variables, Advances in Space Research, https://doi.org/10.1016/j.asr.2019.09.006

Table 1
Parameters of confirmed hard X-ray IPs

Name	P_ω (s)	P_Ω (min)	WD Mass ($M_\odot$)	$F_{X,bol}$[a]	Distance[b] (pc)	References
SWIFTJ0023.2+6142/V1033 Cas	563.5	242.0	$0.91^{+0.14}_{-0.16}$	1.84 ± 0.2	1493^{+137}_{-116}	1,2,3,4
SWIFTJ0028.9+5917/V709 Cas	312.8	320.0	$0.88^{+0.05}_{-0.04}$	11.07 ± 2.2	731^{+12}_{-11}	1,5,6,4
SWIFTJ0055.4+4612/V515 And	465.5	163.9	0.79 ± 0.07	18.6 ± 0.4	978^{+47}_{-42}	1,7,4
SWIFTJ0256.2+1925/XY Ari	206.3	363.9	0.96 ± 0.12	...	...	1,2
SWIFTJ0331.1+4355/GK Per	351.3	2875.4	0.87 ± 0.08	$5.5^{+0.5}_{-0.9}$[c]	437^{+8}_{-10}	1,8,4
SWIFTJ0457.1+4528	1218.7	371.3:	1.12 ± 0.06	3.2 ± 0.2	2000^{+570}_{-556}	9,10,4
SWIFTJ0502.4+2446/V1062Tau	3704	598.9	0.72 ± 0.17	13.90 ± 0.48	1512^{+209}_{-164}	1,6,4
SWIFTJ0524.9+4246/Paloma	7800:	156	...	1.6 ± 0.4	573^{+37}_{-34}	11,4
SWIFTJ0525.6+2416	226.3	...	1.01 ± 0.06	5.0 ± 0.4	1888^{+362}_{-267}	10,4
SWIFTJ0529.2-3247/TV Col	1909.7	329.2	0.78 ± 0.06	25.9 ± 2.0	505^{+5}_{-4}	1,2,6,4
SWIFTJ0543.2-4104/TX Col	1911	343.2	0.67 ± 0.10	10.3 ± 4.2	899 ± 26	1,2,6,4
SWIFTJ0558.0+5352/V405 Aur	545.4	249.6	0.89 ± 0.13	12.5 ± 3.0[d]	662^{+14}_{-13}	1,2,6,4
SWIFTJ0625.1+7336/MU Cam	1187.2	283.1	0.74 ± 0.13	5.0 ± 0.4 [d]	954^{+26}_{-25}	1,2,12,4
SWIFTJ0636.6+3536/V647 Aur	932.9	207.9	0.74 ± 0.06	3.1 ± 0.3	2073^{+339}_{-260}	1,7,4
SWIFTJ0704.4+2625/V418 Gem	480.7	262.8	0.5 ± 0.2	2.46 ± 1.0	2550^{+927}_{-602}	1,13,4
SWIFTJ0731.5+0957/BG CMi	913.5	194.1	0.67 ± 0.19	11.5 ± 0.8	966^{+56}_{-50}	1,2,6,4
SWIFTJ0732.5-1331/V667 Pup	512.4	336.2	0.79 ± 0.11	7.9 ± 1.0	1848^{+178}_{-150}	1,2,4
SWIFTJ0746.3-1608	2311:	562.8	0.78 ± 0.13	1.84 ± 0.06	638 ± 12	14
SWIFTJ0750.9+1439/PQ Gem	833.4	311.6	0.65 ± 0.09	13.9 ± 3.9[d]	750^{+21}_{-20}	1,2,6,4
2PBCJ0801.2-4625	1306.3	...	1.18 ± 0.10	4.8 ± 0.3	1315^{+48}_{-49}	15,4
SWIFTJ0838.0+4839/EI UMa	741.6	386.1	$9.1^{+0.017}_{-0.07}$[e]	4.3 ± 0.9 [e]	1095^{+47}_{-43}	1,4
IGRJ08390-4833/SWIFTJ0838.8-4832	1480.8	480:	0.95 ± 0.08	2.52 ± 0.3	2064^{+311}_{-240}	1,7,4
SWIFTJ0927.7-6945	1033.5	291.0	0.58 ± 0.10	2.7 ± 0.16	1123^{+39}_{-38}	15,16,4
SWIFTJ0958.0-4208	296.2	...	0.74 ± 0.11	2.2 ± 0.13	1586^{+161}_{-134}	15,4
SWIFTJ1142.7+7149/YY Dra	529.3	238.1	0.75 ± 0.02	3.9 ± 0.6	198 ± 1	1,17,6,4
SWIFTJ1238.1-3842/V1025 Cen	2146.6	84.6	$0.60^{+0.06}_{-0.03}$	3.4 ± 0.6	192^{+5}_{-4}	1,18,6, 4
SWIFTJ1252.3-2916/EX Hya	4021.6	98.3	0.78 ± 0.03	13.8 ± 1.0	$56.85^{+0.05}_{-0.13}$	1,19,20,4
IGRJ14091-6108/Swift J1408.26113	576.3	...	1.2–1.3	1.1	2808^{+1157}_{-673}	21,4
IGRJ142576117/4PBCJ1425.1-6118	509.5	243	0.6 ± 0.2	2.19 ± 0.22	1645^{+533}_{-329}	6,4
IGRJ1509-6649/SWIFTJ1509.4-6649	809.4	353.4	0.89 ± 0.08	6.8 ± 0.2	1127^{+37}_{-34}	1,7,4
SWIFTJ1548.0-4529/NY Lup	693.0	591.8	$1.16^{+0.04}_{-0.02}$	17.7 ± 9.7	1228^{+44}_{-40}	1,5,6,4
IGRJ16500-3307/SWIFTJ1649.9-3307	571.9	217.0	0.92 ± 0.06	6.1 ± 0.20	1140^{+88}_{-77}	1,7,4
IGR J16547-1916/SWIFTJ1654.7-1917	546.7	222.9	0.85 ± 0.15	$4.7^{+0.3}_{-1.4}$	1066^{+60}_{-55}	1,22,4
SWIFTJ1701.3-4304/Nova Sco AD 1437	1858.7	769.0	1.16 ± 0.12	41.0 ± 2.5	1014^{+54}_{-48}	15,4
SWIFTJ1712.7-241/V2400 Oph	927.7	205.8	0.81 ± 0.10	28.6 ± 1.8	701^{+17}_{-16}	1,2,6,4
IGRJ1719-4100/SWIFTJ1719.6-4102	1053.7	240.3	0.86 ± 0.06	11.4 ± 0.2	643 ± 17	1,7,4
SWIFTJ1730.4-0558/V2731 Oph	128.0	925.3	1.16 ± 0.05	28.1 ± 0.5	2165^{+316}_{-245}	1,23,24,4
AXJ1740.2-2903	628.6	343.3	...	~1.1	1351^{+1532}_{-474}	1,25,4
IGRJ18173-2509/SWIFTJ1817.4-2510	1663.4	91.9:	0.96 ± 0.05	7.40 ± 0.20	...	1, 4
IGRJ18308-1232/SWIFTJ1830.8-1253	1820.0	322.4	0.85 ± 0.06	19.3 ± 4.0	2074^{+1232}_{-591}	1,7,4
SWIFTJ1832.5-0863/AXJ1832.3-0840	1552.3	...	...	~ 1.54	1051^{+2421}_{-482}	1,26,4
SWIFTJ1855.0-31/V1223 Sgr	745.5	201.9	0.75 ± 0.02	46.0 ± 7.6	571^{+16}_{-15}	1,5,6,4
IGRJ19267+1325	935.1	206.9	...	~2	1443^{+439}_{-276}	1,27,4
IGRJ19552+0044/SWIFTJ1955.2+0077	4877.4	83.6	$0.77^{+0.02}_{-0.03}$	2.20 ± 0.10	170^{+3}_{-2}	28,29,4
SWIFTJ1958.3+3233/V2306 Cyg	1466.7	261.0	0.77 ± 0.16	4.3 ± 0.9[e]	1311^{+61}_{-55}	1,2,4
SWIFTJ2113.5+5422	1265.6	241.2	$0.81^{+0.16}_{-0.10}$	2.9 ± 0.17	547^{+116}_{-82}	15,4
SWIFTJ2123.5+4217/V2069Cyg	743.1	448.8	0.82 ± 0.08	5.20 ± 0.20	1140^{+43}_{-40}	1,7,4
IGRJ21335+5105/SWIFTJ2133.6+5105	570.8	431.6	0.93 ± 0.04	11.9 ± 1.5	1325^{+48}_{-45}	1,3,4
SWIFTJ2217.5-0812/FO Aqr	1254.5	290.9	0.61 ± 0.05	25.38 ± 3.64	518^{+14}_{-13}	1,2,6,4
SWIFTJ2255.4-0309/AO Psc	805.2	215.5	0.55 ± 0.06	15.43 ± 2.33	488^{+11}_{-10}	1,2,6,4

References: (1)P_ω, P_Ω from Ferrario et al. (2015); (2) Brunschweiger et al. (2009); (3) Anzolin et al. (2009); (4) This work, (5) Shaw et al. (2018); (6) Bernardini et al. (2018); (7) Bernardini et al. (2012); (8) Wada et al. (2018); (9) Thorstensen and Halpern (2013); (10) Bernardini et al. (2015); (11) Joshi et al. (2016); (12) Staude et al. (2008); (13) Anzolin et al. (2008); (14)Bernardini et al. (2019a); (15) Bernardini et al. (2017); (16) Halpern et al. (2018); (17) Suleimanov et al. (2005); (18) Ramsay (2000); (19) Echevarría et al. (2016); (20) Luna et al. (2018); (21) Tomsick et al. (2016); (22) Lutovinov et al. (2010), (23) Hailey et al. (2016); (24) de Martino et al. (2008); (25) Masetti et al. (2012), (26) Masetti et al. (2013); (27) Masetti et al. (2009); (28) Tovmassian et al. (2017); (29) Bernardini et al. (2013);

[a] Fluxes in units of 10^{-11} erg cm^{-2} s^{-1}.

[b] Distances obtained from *Gaia* parallaxes and weak distance prior using Galactic model described in (Bailer-Jones et al., 2018). Uncertainties encompass lower and upper bounds of highest posterior probability. Unreliable distances are not reported.

[c] Quiescent flux.

[d] Average flux between two observations.

[e] Obtained from combined *Swift*/XRT and BAT archival spectra retrieved from the products generator at the UK *Swift* Science Data Centre (Evans et al., 2009) and from the NASA/GSFC *Swift*-BAT 105-month Web site https://swift.gsfc.nasa.gov/results/bs105mon/, respectively.

Please cite this article as: D. de Martino, F. Bernardini, K. Mukai et al., Hard X-ray cataclysmic variables, Advances in Space Research, https://doi.org/10.1016/j.asr.2019.09.006

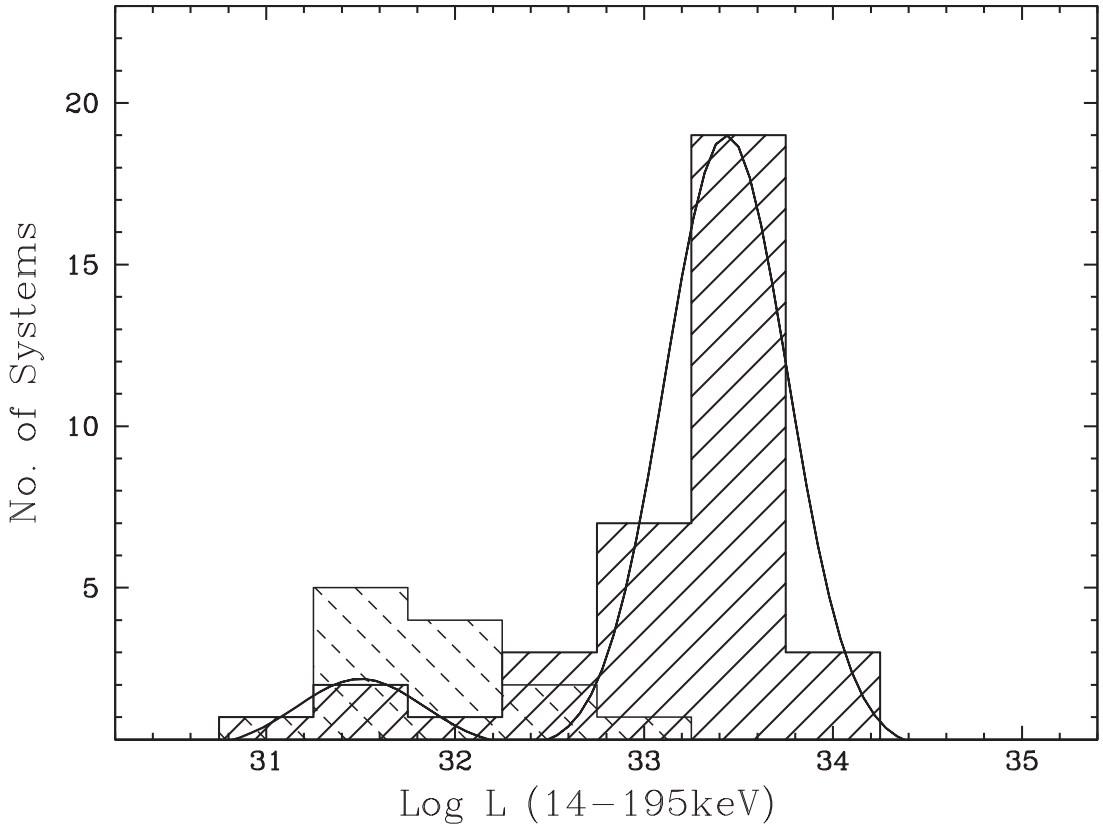

Fig. 2. The 14–195 keV luminosity distribution of confirmed IPs (solid) and polars (dashed) detected in the Swift/BAT survey with Gaia distances accurate better than 10%. A hint of a bimodal distribution (solid line) in the IP sample could be present with four low-luminosity systems overlapping the Polar sample.

2013; Thorstensen et al., 2015) and thus subject of revisions (Fig. 1). Optical photometry may unveil coherent pulsations, although these do not unambiguously identify the rotation period of the accreting WD (see Section 3.1). Other cases occur when intermittent optical short-period variations are present that hamper a secure classification. The detection of X-ray pulses and spectral characteristics instead efficiently diagnose the magnetically channeled accretion flow onto the WD primary and thus allow firm confirmation of the magnetic status of candidates.

With a long-term programme using *XMM-Newton* we could confirm the magnetic status of 29 CVs, of which 26 resulted IP-type systems (see Bernardini et al., 2012, 2013, 2017, 2018, 2019a, and references therein) and 3 of them were found to be hard X-ray polars (Bernardini et al., 2014, 2017, 2019b). We also disproved the mCV nature of 6 systems, due to the lack of X-ray pulsations although for two of them X-ray spectra closely resemble those of IPs (Bernardini et al., 2013, 2019c,in prep). Noteworthy is the case of a bright hard X-ray low-mass X-ray binary, XSS J12270-4859, associated by us to a *Fermi*-LAT gamma-ray source, previously misidentified as an IP and later recognized as one of the few intriguing transitional millisecond pulsar binaries (see de Martino et al., 2010, 2013).

The current roster of confirmed IPs amounts to 69 systems with 50 detected as hard X-ray sources (see Table 1 for a complete list of hard IPs as of September 2018).[2] The increase in number of confirmed hard polars to 13, out of ~130 (Ritter and Kolb, 2003, update RKcat7.24,2016), suggests they are not as rare as previously thought.

3.1. Timing properties of identified mCVs

The marking characteristics of mCVs is the presence of an X-ray periodic modulation at the spin period of the WD. Therefore the synchronous polar systems are known to display marked (up to ~ 100%) variability at the orbital (~hrs) period due to the self-occultation of the accretion spot behind the limb of the WD, giving rise to bright and faint phases (see reviews by Cropper, 1990; Mukai, 2017)[3]. The hard polars identified in our programme, Swift J2218.4+1925, Swift J0706.8+0325 and Swift-J0658.0-1746, display similar modulation (Bernardini et al., 2014, 2017, 2019b) with the faint phases not reaching zero counts, indicating the presence of a secondary accreting pole. In two of them energy dependend orbital light

[2] Known and candidate systems can be found at https://asd.gsfc.nasa.gov/Koji.Mukai/iphome/iphome.html.

[3] A handful of polars are found to be slightly ($\lesssim 2\%$) desynchronised, displaying also long-term variations at the sideband orbital frequency $\omega - \Omega$ (see Ferrario et al., 2015; Rea et al., 2017, and references therein)

curves are characterised by a narrow dip overimposed on the bright phase, a common feature of polars, due to photoelectric absorption when the accretion stream intercepts the line of sight (e.g. Ramsay et al., 2004). In Swift J2218.4+1925 this feature does not disappear at higher energies (>2 keV) and is similar to the rare case of EP Dra (e.g. Ramsay et al., 2004), indicating that there is a dense core obscuring the accretion region. No soft X-ray additional component appears to be present in these new polars (see also Section 3.2). These systems are likely low-field polars ($\sim 7-14\times10^6$ G) (see details in Bernardini et al., 2014, 2017).

IPs instead display much faster periodic variability. Generally, the spin (P_ω) period dominates their X-ray power spectra indicating accretion occurs via a disc (Wynn and King, 1992; Norton et al., 1996). The presence of sidebands and particularly a strong beat periodicity ($P_{\omega-\Omega}$) is the hallmark of a disc-overflow accretion (Hellier, 1995; Norton et al., 1996, 1997). Only one system, V2400 Oph is known to date to display strong X-ray pulsations at the beat period, thus representing a unique case among IPs where accretion onto the WD occurs withouth an intervening disc (Buckley et al., 1997; de Martino et al., 2004).

The new IPs also show a dominant spin periodicity (Anzolin et al., 2009; Bernardini et al., 2012, 2013, 2015, 2017, 2018), with a few also displaying weaker power at the harmonic of the spin frequency in their power spectra, indicating the presence of a secondary weakly emitting pole. Remarkable is the case of IGR J1817-2509, a pure two-pole accretor, displaying X-ray pulses only at 2ω (Bernardini et al., 2012). These systems are then disc-accretors, where the material from the disc attaches to the magnetic field lines and is channeled onto the WD magnetic poles in an arc-shaped curtain (Rosen et al., 1988). In this configuration the maximum of the pulsation is observed when the curtain points away from the observer and when the optical depth of the accretion funnel is minimum (Rosen et al., 1988; Norton and Watson, 1989; Norton et al., 1999). Most IPs have therefore the energy dependent spin pulses with amplitudes increasing at lower energies, indicative of photoelectric absorption along the pre-shock accretion flow. The absorbing material partially covers the X-ray emitting region and it is complex, requiring a distribution of covering fraction as a function of column density (see details in Done and Magdziarz, 1998; Mukai, 2017). Few exceptions are those low accretion rate IPs where absorption in the pre-shock flow is negligible and thus the spin modulation is mainly due to changes in the visible portion of the emitting region (e.g. Allan et al., 1998; de Martino et al., 2005). It has also to be noted that those few systems observed at energies $\geqslant10$ keV at adequate S/N, such as with *NuSTAR*, have shown hard X-ray spin pulses that cannot be ascribed to absorption, implying non-negligible shock heights (de Martino et al., 2001; Mukai et al., 2015).

Noteworthy is the high incidence ($\sim45\%$) of systems found to be spin-dominated in the X-rays but dominated by the beat in the optical band (Bernardini et al., 2012), implying that the optical light is affected by reprocessing at fixed regions in the binary frame. This also demonstrates that optical pulses are not reliable tracer of the WD rotation. Many of the identified IPs have been found to also display non-negligible variability at the beat ($\omega-\Omega$) frequency in the X-rays, which, in a few cases, can reach amplitudes as large as those of the spin modulation (e.g. Bernardini et al., 2017). These systems have an hybrid geometry where substantial portion of the accreting matter overflows the disc and directly impacts onto the WD magnetosphere.

The long uninterrupted exposures with *XMM-Newton* increased the number of IPs displaying substantial X-ray orbital variability. A few (8 so far) are eclipsing IPs, giving the opportunity to study in details the accretion geometry (see Hellier, 2014; Esposito et al., 2015; Johnson et al., 2017; Bernardini et al., 2017). Orbital modulations were found to be energy dependent from *ASCA* and *RXTE* observations in 7 systems and interpreted as photoelectric absorption due to material located at the disc rim (Parker et al., 2005). The number of IPs showing energy dependent orbital modulations has now increased to 13 systems (Parker et al., 2005; Bernardini et al., 2012, 2017, 2018). The amplitudes are found to range from 3 to 4% up to $\sim100\%$ as in the extreme cases of FO Aqr, Swift J0927.7-6945 and IGR J14257-6117. Drawing similarities with low-mass X-ray binaries displaying orbital dips, IPs showing large orbital modulations should be seen at moderately high ($\gtrsim60^o$) binary inclinations, allowing azimuthally extended absorbing material to intercept the line of sight (Parker et al., 2005; Bernardini et al., 2018). Changes of the amplitudes with epochs were already detected by Parker et al. (2005) and later confirmed by Bernardini et al. (2018), possibly linked to changes in the mass accretion rate. However, such possibility has not found confirmation yet.

Interesting case is IGR J19552+0044 found to display two close long periods of 1.69 h and 1.35 h interpreted as the orbital and spin periods, respectively (Bernardini et al., 2013). These have been recently improved with a long optical campaign resulting in $P_\Omega=1.393$ h and $P_\omega=1.355$ h (Tovmassian et al., 2017). The spin-to-orbit period ratio is remarkably high, $P_\omega/P_\Omega=0.97$ making IGR J19552+0044 the IP with the lowest degree of asynchronism, and joining "Paloma" which has a spin-to-orbit period ratio ~0.83 (Joshi et al., 2016). These two systems are likely in their way to become polars and represent test cases for mCV evolution.

3.2. Spectral properties of identified mCVs

The structure of the PSR has been the subject of many studies over the years. Detailed one-dimensional two-fluid

Please cite this article as: D. de Martino, F. Bernardini, K. Mukai et al., Hard X-ray cataclysmic variables, Advances in Space Research, https://doi.org/10.1016/j.asr.2019.09.006

hydrodynamic calculations coupled with radiative transfer equations for cyclotron and Bremsstrahlung were performed for different regimes, including the so-called bombardment regime occurring at very low local mass accretion rates and at high magnetic field strengths (Woelk and Beuermann, 1996; Fischer and Beuermann, 2001). In the latter case a standing shock does not develop and the WD atmosphere is heated from below by particle bombardment. Many X-ray spectral models of mCVs have been developed that account for temperature and gravity gradients, for cyclotron cooling (in the polars), solving one or two-fluid hydrodinamic equations and dipolar field geometry (see Wu et al., 1994; Cropper et al., 1999; Canalle et al., 2005; Saxton et al., 2007; Hayashi and Ishida, 2014). Modifications in the models to account for finite size of magnetosphere, especially in the low-field IPs, have recently been performed to obtain more reliable mass estimates (Suleimanov et al., 2016; Suleimanov et al., 2019).

The mCV spectra are characterised a by multi-temperature optically thin plasma, signified by the presence of the 6–7 keV iron complex with H-like FE XXVI (6.9 keV) and He-like FE XXV (6.7 keV) K_α lines as well as weaker K-shell features of less heavier elements, plus a neutral Fe K_α fluorescent component. The modeling of the X-ray spectra allows tracing temperatures from ~0.2 keV up to ~20–40 keV in the PSR, although a continuous distribution is not always required (e.g. de Martino et al., 2008; Anzolin et al., 2009) indicating that indeed the emergent spectrum is highly sensitive to local pressure and temperature across the flow. Additionally a Compton reflection continuum component emerging at high energies and arising from the WD surface was investigated by Suleimanov et al. (2008) and found to be unimportant for low WD masses and/or for low mass accretion rates. Recently, stringent constraints on the presence of a Compton reflection hump in mCVs have been found using *NuSTAR* observations of three bright hard X-ray IPs (Mukai et al., 2015). This component is usually not required in the spectral fits to the low S/N average BAT and/or IBIS-ISGRI spectra of most IP systems. Reflection either at the WD surface or in the pre-shock flow is anyway confirmed by the above mentioned fluorescent Fe at 6.4 keV (Ezuka and Ishida, 1999), found to be ubiquitous in the spectra of mCVs, with equivalent widths (EW) in the range ~100–250 eV. In a few systems, spin-phase resolved spectra show an increase in the EW at spin minimum, indicating an origin at the WD surface (Bernardini et al., 2012, 2017).

Modeling of X-ray spectra of mCVs, especially the IPs, also requires complexities at low energies, due to the presence of complex absorption from neutral material located in the pre-shock flow with column densities reaching values as high as $\sim 10^{23}\,\mathrm{cm}^{-2}$ (see discussion in Mukai, 2017). Phase-resolved spectroscopy of these systems including the newly identified mCVs indeed reveals that the partial covering fraction of the local absorber changes along the spin cycle producing the observed energy dependence of spin pulses (e.g. Bernardini et al., 2012, 2017). An additional absorption component is required in those IPs displaying energy dependent orbital modulations (Bernardini et al., 2012, 2018). While mCVs were not previously known to show ionized absorption features in their X-ray spectra, *XMM-Newton* and *Chandra* grating spectra have demonstrated at least in three IPs the presence of an OVII absorption edge (Mukai et al., 2001; de Martino et al., 2008; Bernardini et al., 2012). This indicates that in some IPs the pre-shock flow can be also substantially ionized.

Additionally, an optically thick soft (~20–60 eV) component, arising from the heated polar cap, was believed to be the characterising spectral feature of polars (Beuermann, 1999), but not of IPs, except a handful of "soft" IP systems (Haberl and Motch, 1995; Haberl et al., 2002; de Martino et al., 2004). *XMM-Newton* has remarkably shown an increasing number of polars without a distinct soft X-ray excess (Ramsay and Cropper, 2004; Ramsay et al., 2004, 2009; Bernardini et al., 2014, 2017; Worpel et al., 2016), suggesting that if a reprocessed component exist, this has a low temperature shifting the emission towards the EUV/UV ranges. This also implies that polars cannot be characterised as soft X-ray emitting sources anymore. Thanks to the high sensitivity of *XMM-Newton* the number of IPs showing a soft blackbody component has remarkably increased from the three *ROSAT*-discovered systems to 19, representing ~ 30% of the whole IP class (see details in Anzolin et al., 2008; Bernardini et al., 2017). Among them 8 are found to be polarised in the optical/nIR band (Ferrario et al., 2015; Potter and Buckley, 2018), possibly suggesting that the detectability of the soft X-ray component could be linked to the additional contribution of cyclotron radiation in the reprocessing at the WD surface ($L_{BB} \sim L_{X,hard} + L_{cyc.}$). The soft X-ray blackbody temperature are found to span a wider range from ~40 eV up to ~100 eV with very different soft-to-hard X-ray luminosity ratios (see Fig. 3), but on average lower than those inferred in the soft polars. The inferred fractional areas are much smaller than those typically found in polars by two-three orders of magnitudes. Although high blackbody temperatures arising from the WD surface would be locally super-Eddington, the possibility that the soft component originates instead in the coolest regions of the PSR above the WD surface is not supported by the spectral fits (Bernardini et al., 2017). It could be also possible that, as demonstrated in the polar prototype AM Her, there is a temperature gradient over a large area of the polar cap (Beuermann et al., 2012), with the inner core regions reaching such high temperatures. In the case of IPs, the hotter regions are detectable against the high absorbing column rather than the cooler and softer ones. Here we also note that due to the arc-shaped nature of the accretion spot in IPs, the structure of the heated area at the WD photosphere is likely to be different than that in the polars.

Please cite this article as: D. de Martino, F. Bernardini, K. Mukai et al., Hard X-ray cataclysmic variables, Advances in Space Research, https://doi.org/10.1016/j.asr.2019.09.006

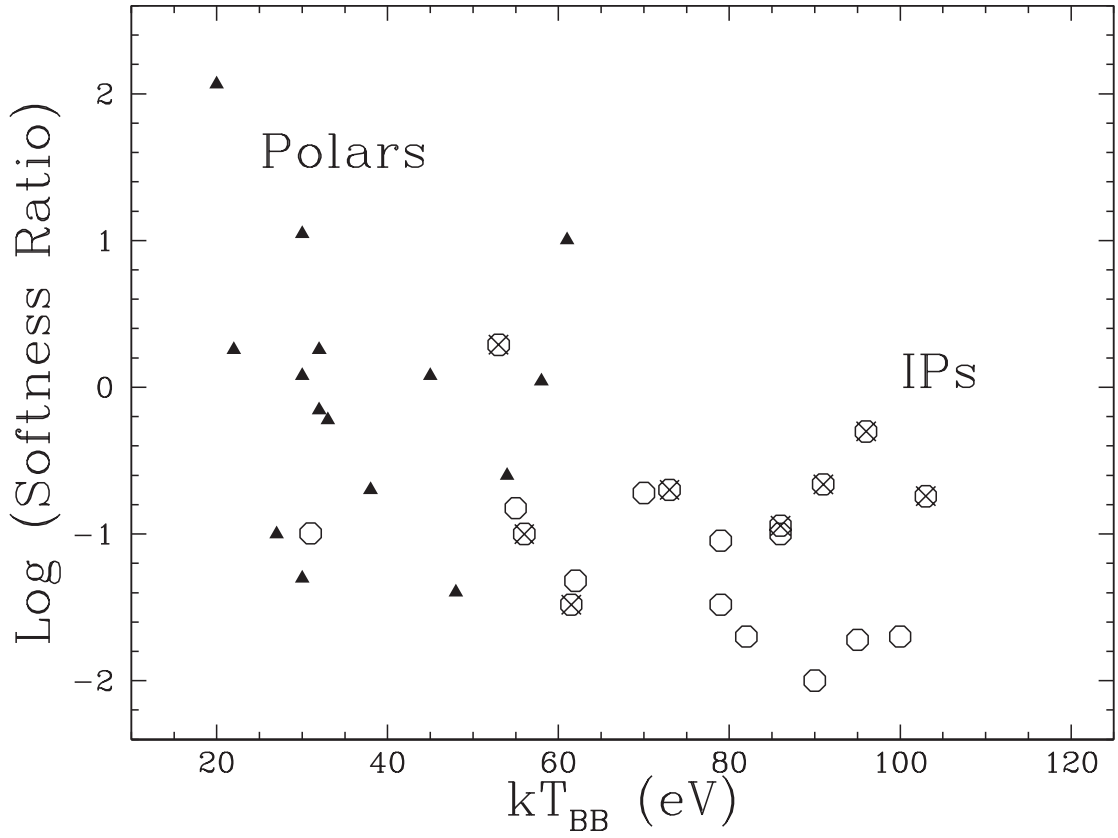

Fig. 3. The softness ratio of polars (filled triangles) and of soft IPs (open circles) versus blackbody temperature. The polarised IPs are also marked with a cross. Adapted from Bernardini et al. (2017).

4. The role of fundamental parameters

We here discuss some of the fundamental parameters obtained from the enlarged sample of IPs.

4.1. The spin-orbit period plane of IPs

In Fig. 4 the spin-orbit period plane of the 69 confirmed IPs with determined orbital periods is displayed together with the corresponding spin and orbital period distributions. Previously known IPs were concentrated in a limited range of the spin-orbit period plane, clustering just below $P_\omega/P_\Omega \sim 0.1$ with most systems found above the 2–3 h orbital period gap, typically in the range 3–6 h. With the new identifications the plane has been substantially populated at long periods with 15 systems at $P_\Omega > 6$ h. Among them two are old novae, GK Per and SWIFT J1701.3-4304, recently identifed as Nova Sco AD 1437 (Shara et al., 2017; Bernardini et al., 2017). The new long period (P_Ω = 12.8 h) IP, RX J2015.6+3711, still with an ambiguous identification in hard X-rays, is worth mentioning for its extremely slow rotation (P_ω=2 h) (Coti Zelati et al., 2016; Halpern et al., 2018), only surpassed by "Paloma". These very long orbital period IPs represent ∼ 10% of the whole CV population in this period range. Long period systems are believed to enter in the CV phase with nuclear evolved donors and may represent a significant portion of the present-day CV population (Beuermann et al., 1998; Goliasch and Nelson, 2015). Their spin-orbit period ratios, suggest they will reach synchronism while evolving to short orbital periods. On the short period side, the number of IPs below the 2–3 h CV orbital period gap has surprisingly increased to 10 members (Fig. 4). This is challenging since short period mCVs should have already reached synchronism if their magnetic moments are greater than $\sim 5 \times 10^{33}$ G cm^3 (see Norton et al., 2004, 2008). The large spread in spin-to-orbit period ratios of these short period IPs may suggest they belong to a different population of old, possibly, very low-field systems that will never synchronise.

The spin-orbit period ratios observed in IPs were investigated in terms of their complex accretion geometry. Norton et al. (2004, 2008) showed that if the WDs in IPs are spinning at equilibrium, systems with very small spin-orbit period ratios ($P_\omega/P_\Omega \lesssim 0.1$) should accrete via a disc, while those ratios between 0.1 and 0.6 would be accreting via disc/stream, depending on the binary mass ratio, and reaching a ring-like configuration at $P_\omega/P_\Omega \sim 0.6$. Those IPs with higher spin-orbit period ratios should be far from equilibrium.

Please cite this article as: D. de Martino, F. Bernardini, K. Mukai et al., Hard X-ray cataclysmic variables, Advances in Space Research, https://doi.org/10.1016/j.asr.2019.09.006

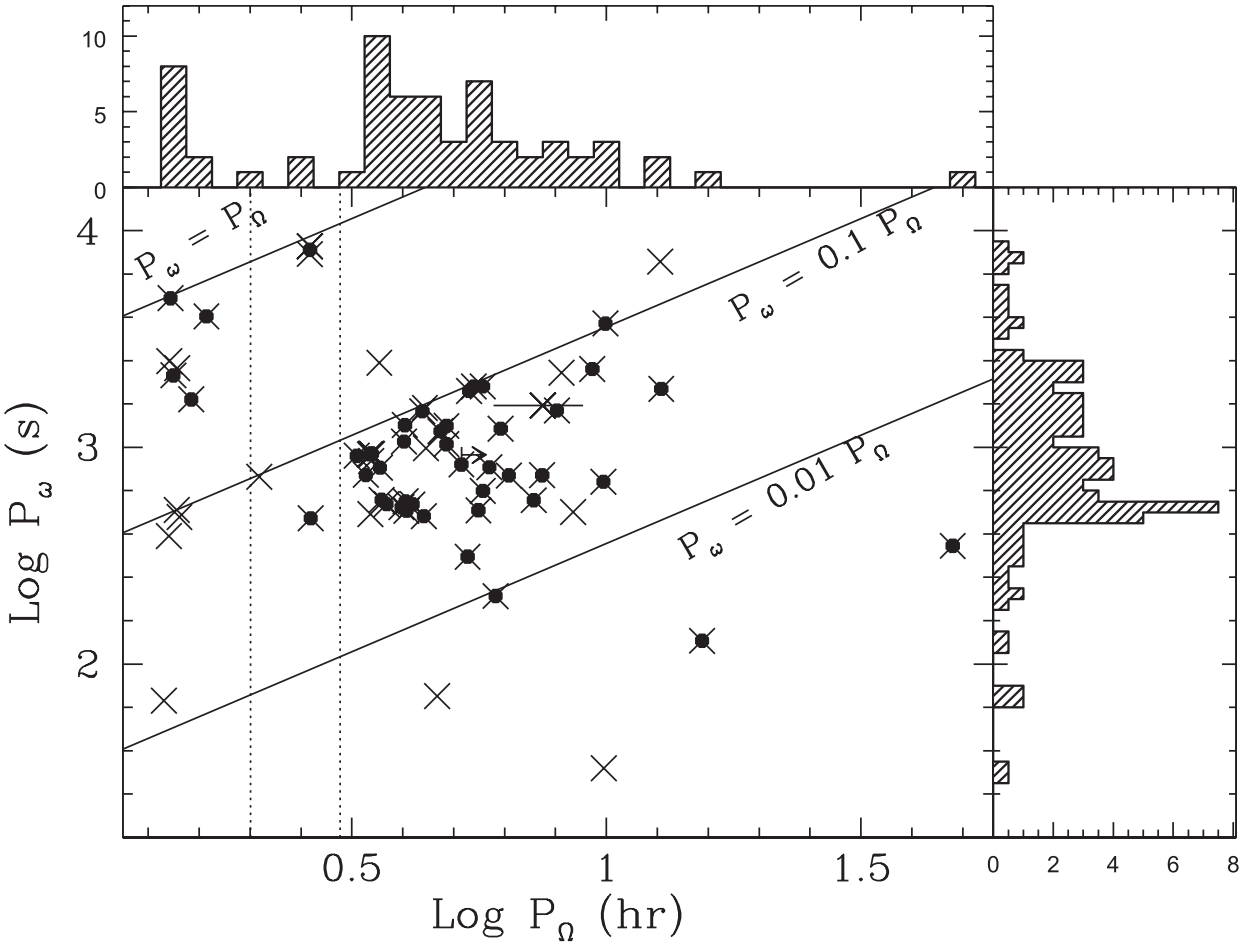

Fig. 4. The spin-orbit period plane of confirmed IPs (crosses). Hard X-ray detected sources are also shown as filled circles. Solid lines mark synchronism and two levels of asynchronism (0.1 and 0.01). Vertical lines mark the orbital CV gap, where mass transfer is expected to stop at the upper bound and to be resumed at the lower bound. The spin (right panel) and orbital (upper panel) period distributions are reported (adapted from Bernardini et al. (2017), including Bernardini et al. (2018, 2019a)).

4.2. The mass distribution of hard X-ray IPs

The broad-band X-ray spectra of mCVs identified in our programme, obtained combining *XMM-Newton* and *Swift*/BAT or *INTEGRAL*/IBIS-ISGRI data, increased the sample of IP systems for which the WD mass has been estimated (Bernardini et al., 2012, 2013, 2017, 2018, 2019a). These determinations are based on the PSR model by Suleimanov et al. (2005). This model, and similar methods based on multi-temperature fit, have also been applied to the previously known bright hard IPs identified in the first 2.5 yrs of *Swift*/BAT survey (Brunschweiger et al., 2009) and to a few of them recently re-observed in the hard X-rays at much higher S/N with *NuSTAR* (Tomsick et al., 2016; Hailey et al., 2016; Shaw et al., 2018; Wada et al., 2018). The WD mass distribution of 46 hard X-ray IPs is shown in the left upper panel of Fig. 5, with a mean value $< M_{WD} >= 0.84 \pm 0.17\,M_{\odot}$. The modified PSR model accounting for the finite size of the magnetosphere was also recently applied to a set of 35 IPs observed with *NuSTAR* and *Swift*/BAT by Suleimanov et al. (2019), who find more accurate WD masses with an average value of $0.79 \pm 0.16\,M_{\odot}$, but still consistent with previous results. Massive WD primaries were also found by Zorotovic et al. (2011), using a set of "fiducial" CVs with reliable WD masses (left middle panel of Fig. 5) with a mean value $< M_{WD,fiducial} >= 0.82 \pm 0.15 M_{\odot}$. Similar results are found using the WD masses listed in the Ritter and Kolb (2003, update RKcat7.24,2016) catalogue of CVs (left bottom panel of Fig. 5). We performed a Kolmogorov-Smirnov (K-S) test between the masses of hard X-ray IPs and those of fiducial CVs, resulting in a probability of 99.3% that the distributions are from the same parent population (right panel of Fig. 5). Hence, irrespective of being magnetic or not, WD primaries in CVs are more massive than single WDs ($0.6\,M_{\odot}$) and WDs in pre-CV binaries ($0.67\,M_{\odot}$). This could suggest that WDs in CVs grow in mass during their evolution (see Zorotovic et al., 2011), and that CVs may be favourable SN Ia progenitors. This result however strongly disagrees with the predictions of classical nova models (e.g. Prialnik and Kovetz, 1995). Whether novae gain or loose mass is still highly

Please cite this article as: D. de Martino, F. Bernardini, K. Mukai et al., Hard X-ray cataclysmic variables, Advances in Space Research, https://doi.org/10.1016/j.asr.2019.09.006

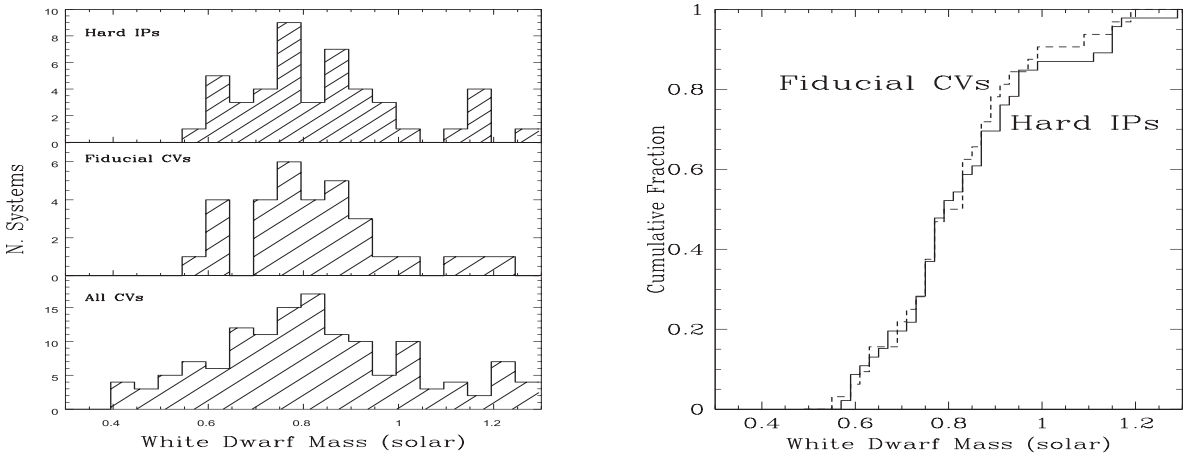

Fig. 5. Left panel: The distributions of the WD masses of hard IPs (up) listed in Table 1, of the fiducial CVs taken from Zorotovic et al. (2011) (middle) and those listed in the Ritter and Kolb (2003, update RKcat7.24,2016) catalogue of CVs (bottom). *Right panel:* The cumulative distributions of the mass of hard X-ray IPs (solid line) and the mass of the fiducial CVs (dashed line).

controversial (Yaron et al., 2005; Starrfield et al., 2009) since the determination of the ejected mass is extremely challenging see Shara et al. (2010, 2015).

We also note that the mean mass of high field isolated magnetic WDs ($B \gtrsim 10^6$ G) is $0.78 \pm 0.05\,M_\odot$ very different from the mean mass of single WDs (Ferrario et al., 2015). The fact that no magnetic WD is found in detached MS +WD binaries led Tout et al. (2008) and later Wickramasinghe et al. (2014) to propose the possibility that the strong differential rotation expected to occurr during the commone envelope (CE) phase may lead to the generation, by the dynamo mechanism, of a magnetic field that becomes frozen into the degenerate core of the pre-WD in MCVs making these binaries hardly detectable. It is expected that at the end of the CE phase CV systems with smaller orbital separations have WDs with stronger magnetic fields. Those systems that instead do merge are the progenitors of the single high field WDs.

4.3. The mass accretion rate

The study of the broad-band spectra of IPs allows a derivation of the X-ray bolometric luminosity, also accounting for the reprocessed X-ray emission in the soft IPs. The main uncertainty in previous luminosity determinations was the distances, generally estimated with indirect methods (e.g. Bernardini et al., 2012, 2017). With the *Gaia* DR2 parallax release it has been possible to obtain reliable distances. Most of the mCVs are found to be at a larger distance than previously determined. We have used a sample of 43 hard IPs with known orbital periods, distances and determined bolometric fluxes, reported in Table 1. To evaluate the uncertainty in the luminosities we account for the errors in the derived 0.1–100 keV X-ray fluxes and, when not available we account for a 30% uncertainty, and use the upper and lower bounds of distances derived with the method reported in Bailer-Jones et al. (2018). In Fig. 6 (left

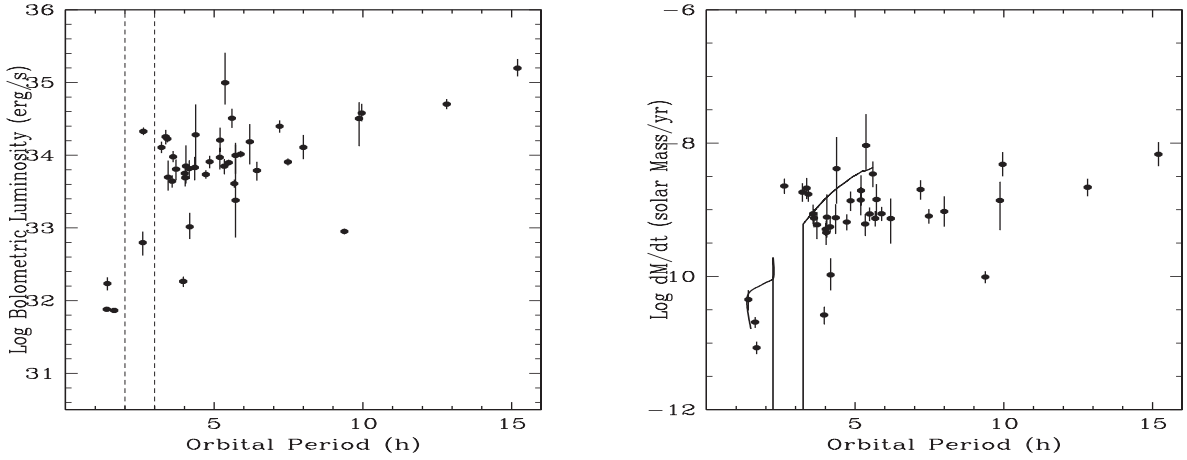

Fig. 6. *Left panel:* The X-ray bolometric luminosities of 43 hard X-ray IPs with known orbital period, obtained using X-ray fluxes and distances reported in Table 1. The dashed vertical lines mark the 2–3 h period gap. *Right panel:* The mass accretion rates versus P_Ω as derived from the bolometric luminosities and adopting the WD masses reported in Table 1 for 39 IPs. The solid line represent the revised CV evolutionary sequence by Knigge et al. (2011) for an assumed WD mass of $0.75 M_\odot$.

Please cite this article as: D. de Martino, F. Bernardini, K. Mukai et al., Hard X-ray cataclysmic variables, Advances in Space Research, https://doi.org/10.1016/j.asr.2019.09.006

panel), we show the luminosities for this sample of IPs as a function of the orbital period up to 16 h (only GK Per is out of the graph). The long period systems, as expected, have larger luminosities by two orders of magnitude than the short period ones. This suggests that, if the X-rays trace the mass accretion rate, their bolometric luminosities could be considered as proxies of the accretion luminosity. However, the UV/optical light in IPs may carry a non-negligible fraction of X-ray reprocessed flux (see Mukai et al., 1994) and thus the results have to be taken with caution. Assuming $L_{X,Bol.} \sim L_{acc} = G M_{WD} \dot{M} R_{WD}^{-1}$ and using the WD masses reported in Table 1 and the M-R relation by Nauenberg (1972), we derive the mass accretion rates for a sample of 39 systems. These rates versus P_Ω are shown in the right panel of Fig. 6, together with the revised evolutionary sequence for an assumed WD mass of $0.75 M_\odot$ obtained by Knigge et al. (2011), adopting a scaled version of angular momentum loss (AML) recipes for magnetic braking and gravitational radiation. While for the polars the magnetic coupling between the primary and the donor could be important in reducing the efficiency of magnetic braking, thus lowering the mass accretion rate (Wickramasinghe and Wu, 1994; Wickramasinghe and Ferrario, 2000; Ferrario et al., 2015), for the asynchronous IPs this effect might not be important. The decrease in mass accretion rate towards short orbital periods is broadly consistent with CV evolutionary theories (Howell et al., 2001; Andronov et al., 2003; Knigge et al., 2011), although the long-period systems appear to have lower rates than the predicted secular values. This was also noticed in non-magnetic CVs using the effective WD temperature, $T_{WD,eff}$, which is a more robust $\dot{M}$-proxy (Pala et al., 2017). Whether the accretion light or $T_{WD,eff}$ are reliable tracers of donor mass transfer rates is matter of debate (Knigge et al., 2011). The newly identified systems at very long periods, $P_\Omega > 6$ h, should have donors that are nuclear evolved. Very long orbital period CVs might represent a non-negligible fraction of present-day CV population still to be identified (Goliasch and Nelson, 2015).

Two long period systems, YY Dra and Swift J0746.3-1608 stick below the bulk of IPs, indicating they have been caught in a low or intermediate luminosity state. However, the majority of IPs are persistent systems. Exceptions are EX Hya, HT Cam, XY Ari, YY Dra and GK Per that display occasional dwarf nova outbursts lasting a few days except for GK Per whose outbursts last a few months. TV Col and V1223 Sgr have instead shown hrs-long outbursts (see Szkody et al., 2002; Hellier, 2014, and references therein). These outbursts are due to disc instabilities. In Fig. 6 none of them are reported during outburst.

Two IPs, AO Psc and V1223 Sgr have instead shown low accretion states in the past, with V1223 Sgr remarkably dimming for about a decade (Garnavich and Szkody, 1988). Their orbital periods fall in the 3–4 h range where VY Scl stars, the novalike systems undergoing deep low states, are found (see Rodríguez-Gil et al., 2007). The orbital period of YY Dra (3.96 h) falls in the same range. As for systems outside the VY Scl period range, the longer period (4.85 h) IP, FO Aqr, was persistently observed at about the same level for several decades until 2016 when it underwent three low states in about 2 yrs (Kennedy et al., 2017b; Littlefield et al., 2018). Littlefield et al. (2019) additionally find two low states occurring in the late 60-ties and mid 70-ties. The very long period (9.38 h) system Swift J0746.3-1608 could not be identified as an IP in an *XMM-Newton* observation in 2016 (Bernardini et al., 2017) due to its extreme faintness in the X-rays. It has been recently identified in 2018, when it recovered a strongly variable higher state after a possibly 6yrs-long faint X-ray level (Bernardini et al., 2019a). Its position in the $\dot{M}$-P_Ω plane suggests that it was still in a sub-luminous state in 2018. The low states are believed to be due to a temporary reduction of the mass transfer rate from the donor star (Livio and Pringle, 1994), causing the accretion disc to be dissipated once the mass transfer drops below a critical threshold (Hameury and Lasota, 2017). In the well studied case of FO Aqr both the X-ray and optical/UV modulations were found to vary in amplitude over the years and also during the recent low states. This indicates that changes in the accretion mode are also likely driven by mass transfer rate variations (Beardmore et al., 1998; de Martino et al., 1999; Kennedy et al., 2017a; Littlefield et al., 2019). State transitions, although rare in IPs, are an important new aspect to understand angular momentum loss governing the evolution of mCVs towards short orbital periods.

5. Discussion and conclusions

We have presented the main results of an ongoing identification X-ray programme of new mCVs discovered in the *INTEGRAL*/IBIS-ISGRI and *Swift*/BAT surveys, that almost doubles the current roster of IP-type systems and adds three new systems to the small group of hard X-ray polars.

Whether IPs are easily identified in these hard X-ray surveys because of massive WD primaries cannot be confirmed from their mass distribution, which results to be similar to that of other CVs. As demonstrated by Fischer and Beuermann (2001), the PSR flow is one-fluid plasma in presence of moderate magnetic field strengths ($B \lesssim 30 \times 10^6$ G) and high flow rates ($\dot{m} \gtrsim 1 - 5\,g\,cm^{-2}\,s - 1$), where radiative losses are mainly via Bremsstrahlung rather than cyclotron. It is then concievable that not only the IPs but also those polars with high local mass accretion rates can be detected in the harder X-ray bands. While nowdays the multi-temperature structure of the PSR in mCVs can be efficiently diagnosed in the brighter systems through grating spectra, the foreseen ESA large mission *Athena* (Nandra et al., 2013) will routinely perform such studies for a large number of fainter systems as well as precisely measure WD

Please cite this article as: D. de Martino, F. Bernardini, K. Mukai et al., Hard X-ray cataclysmic variables, Advances in Space Research, https://doi.org/10.1016/j.asr.2019.09.006

masses via gravitational redshifts of Fe line. The increasing number of polars without a soft X-ray excess and of IPs displaying a soft optically thick component indicates that the previous separation between the two subclasses based on this spectral characteristics is no longer valid.

The new idenfications have allowed to enlarge the range of orbital periods of IPs, with 10 systems below the gap and 15 above the poorly explored range $P_\Omega \gtrsim 6$ h. A wide range of spin-orbit period ratios is found, with most short-period IPs below the 2–3 h gap possessing a weak degree of asynchronism. These IPs may represent a faint population of very weakly magnetised systems that will likely never synchronise. The advent of sensitive near-future survey experiments as *eROSITA* (Merloni et al., 2012) or planned such as *eXTP* (in't Zand et al., 2019) and *Theseus* (Amati et al., 2018) will have a crucial role in unveling the true population of mCVs and in monitoring their still unexplored long-term X-ray behaviour.

Acknowledgments

This work has been presented at the 42nd COSPAR Assembly in 2018 in Pasadena, USA, at the Session entitled "Nova Eruptions, Cataclysmic Variables and related systems: Observational vs. theoretical challenges in the 2020 era. This work is based on data obtained with *XMM-Newton* and *INTEGRAL*, ESA science missions with instruments and contributions directly funded by ESA Member States, with *Swift*, a NASA science missions with Italian participation, with *NuSTAR*, a NASA science mission and with *Gaia*, an ESA mission, whose data are processed by the Data Processing and Analysis Consortium (DPAC). DdM acknowledges financial support from INAF-ASI agreement I/037/12/0, ASI-INAF contract n.2017-14-H.0 and INAF-PRIN SKA/CTA Presidential Decree 70/2016. FB is founded by the European Unions Horizon 2020 research and innovation programme under the Marie Sklodowska-Curie grant agreement n. 664931. NM acknowledges financial support from ASI-INAF contract n.2017-14-H.0.

References

Aizu, K., 1973. X-ray emission region of a white dwarf with accretion. Prog. Theor. Phys. 49, 1184–1194. https://doi.org/10.1143/PTP.49.1184.

Allan, A., Hellier, C., Beardmore, A., 1998. ASCA X-ray observations of EX Hya – spin-resolved spectroscopy. MNRAS 295, 167–176. https://doi.org/10.1046/j.1365-8711.1998.29511353.x.

Amati, L., O'Brien, P., Götz, D., Bozzo, E., Tenzer, C., Frontera, F., Ghirlanda, G., Labanti, C., Osborne, J.P., Stratta, G., Tanvir, N., Willingale, R., Attina, P., Campana, R., Castro-Tirado, A.J., Contini, C., Fuschino, F., Gomboc, A., Hudec, R., Orleanski, P., Renotte, E., Rodic, T., Bagoly, Z., Blain, A., Callanan, P., Covino, S., Ferrara, A., Le Floch, E., Marisaldi, M., Mereghetti, S., Rosati, P., Vacchi, A., D'Avanzo, P., Giommi, P., Piranomonte, S., Piro, L., Reglero, V., Rossi, A., Santangelo, A., Salvaterra, R., Tagliaferri, G., Vergani, S., Vinciguerra, S., Briggs, M., Campolongo, E., Ciolfi, R., Connaughton, V., Cordier, B., Morelli, B., Orlandini, M., Adami, C., Argan, A., Atteia, J.-L., Auricchio, N., Balazs, L., Baldazzi, G., Basa, S., Basak, R., Bellutti, P., Bernardini, M.G., Bertuccio, G., Braga, J., Branchesi, M., Brandt, S., Brocato, E., Budtz-Jorgensen, C., Bulgarelli, A., Burderi, L., Camp, J., Capozziello, S., Caruana, J., Casella, P., Cenko, B., Chardonnet, P., Ciardi, B., Colafrancesco, S., Dainotti, M.G., D'Elia, V., De Martino, D., De Pasquale, M., Del Monte, E., Della Valle, M., Drago, A., Evangelista, Y., Feroci, M., Finelli, F., Fiorini, M., Fynbo, J., Gal-Yam, A., Gendre, B., Ghisellini, G., Grado, A., Guidorzi, C., Hafizi, M., Hanlon, L., Hjorth, J., Izzo, L., Kiss, L., Kumar, P. et al., 2018. The THESEUS space mission concept: science case, design and expected performances. Adv. Space Res. 62, 191–244. doi:https://doi.org/10.1016/j.asr.2018.03.010. arXiv:1710.04638.

Andronov, N., Pinsonneault, M., Sills, A., 2003. Cataclysmic variables: an empirical angular momentum loss prescription from open cluster data. ApJ 582, 358–368. https://doi.org/10.1086/343030, arXiv: 0104265.

Anzolin, G., de Martino, D., Bonnet-Bidaud, J.-M., Mouchet, M., Gänsicke, B.T., Matt, G., Mukai, K., 2008. Two new intermediate polars with a soft X-ray component. A&A 489, 1243–1254. https://doi.org/10.1051/0004-6361:200810402, arXiv: 0808.1499.

Anzolin, G., de Martino, D., Falanga, M., Mukai, K., Bonnet-Bidaud, J.-M., Mouchet, M., Terada, Y., Ishida, M., 2009. Broad-band properties of the hard X-ray cataclysmic variables IGR J00234+6141 and 1RXS J213344.1+510725. A&A 501, 1047–1058. https://doi.org/10.1051/0004-6361/200911816, arXiv: 0905.1080.

Bailer-Jones, C.A.L., Rybizki, J., Fouesneau, M., Mantelet, G., Andrae, R., 2018. Estimating distance from parallaxes. IV. Distances to 1.33 Billion Stars in Gaia Data Release 2. AJ 156, 58. https://doi.org/10.3847/1538-3881/aacb21, arXiv: 1804.10121.

Barlow, E.J., Knigge, C., Bird, A.J., J Dean, A., Clark, D.J., Hill, A.B., Molina, M., Sguera, V., 2006. 20–100 keV properties of cataclysmic variables detected in the INTEGRAL/IBIS survey. MNRAS 372, 224–232. https://doi.org/10.1111/j.1365-2966.2006.10836.x, arXiv: 0607473.

Beardmore, A.P., Mukai, K., Norton, A.J., Osborne, J.P., Hellier, C., 1998. The changing X-ray light curves of the intermediate polar FO Aquarii. MNRAS 297, 337–347. https://doi.org/10.1046/j.1365-8711.1998.01382.x.

Bernardini, F., de Martino, D., Falanga, M., Mukai, K., Matt, G., Bonnet-Bidaud, J.-M., Masetti, N., Mouchet, M., 2012. Characterization of new hard X-ray cataclysmic variables. A&A 542, A22. https://doi.org/10.1051/0004-6361/201219233, arXiv: 1204.3758.

Bernardini, F., de Martino, D., Mukai, K., Falanga, M., 2014. Swift J2218.4+1925: a new hard-X-ray-selected polar observed with XMM-Newton. MNRAS 445, 1403–1411. https://doi.org/10.1093/mnras/stu1819, arXiv: 1409.2257.

Bernardini, F., de Martino, D., Mukai, K., Falanga, M., 2018. IGR J14257–6117, a magnetic accreting white dwarf with a very strong strong X-ray orbital modulation. MNRAS 478, 1185–1192. https://doi.org/10.1093/mnras/sty1090, arXiv: 1804.09899.

Bernardini, F., de Martino, D., Mukai, K., Falanga, M., 2019a. The true nature of Swift J0746.3-1608: a possible Intermediate Polar showing accretion state changes. MNRAS 484, 101–106. https://doi.org/10.1093/mnras/sty3499, arXiv: 1812.09153.

Bernardini, F., de Martino, D., Mukai, K., Falanga, M., Andruchow, I., Bonnet-Bidaud, J.-M., Masetti, N., Buitrago, D.H.G., Mouchet, M., Tovmassian, G., 2013. On the nature of the hard X-ray sources SWIFT J1907.3-2050, IGR J12123–5802 and IGR J19552+0044. MNRAS 435, 2822–2834. https://doi.org/10.1093/mnras/stt1434, arXiv: 1308.1230.

Bernardini, F., de Martino, D., Mukai, K., Falanga, M., Masetti, N., 2019b. 2PBC J0658.0-1746: a hard X-ray eclipsing polar in the orbital period gap. MNRAS 489, 1044–1053. https://doi.org/10.1093/mnras/stz1951, arXiv: 1907.05318.

Bernardini, F., de Martino, D., Mukai, K., Israel, G., Falanga, M., Ramsay, G., Masetti, N., 2015. Swift J0525.6+2416 and IGR J04571+4527: two new hard X-ray-selected magnetic cataclysmic variables identified with XMM-Newton. MNRAS 453, 3100–3106. https://doi.org/10.1093/mnras/stv1673, arXiv: 1507.06442.

Bernardini, F., de Martino, D., Mukai, K., Russell, D.M., Falanga, M., Masetti, N., Ferrigno, C., Israel, G., 2017. Broad-band characteristics of seven new hard X-ray selected cataclysmic variables. MNRAS 470, 4815–4837. https://doi.org/10.1093/mnras/stx1494, arXiv: 1706.04005.

Beuermann, K., 1999. Magnetic cataclysmic variables: the state of the art after ROSAT. In: Aschenbach, B., Freyberg, M.J. (Eds.), Highlights in X-ray Astronomy, MPE Reports, vol. 272, pp. 410–414.

Beuermann, K., Baraffe, I., Kolb, U., Weichhold, M., 1998. Are the red dwarfs in cataclysmic variables main-sequence stars? A&A 339, 518–524, arXiv: astro-ph/9809233.

Beuermann, K., Burwitz, V., Reinsch, K., 2012. A new soft X-ray spectral model for polars with an application to AM Herculis. A&A 543, A41. https://doi.org/10.1051/0004-6361/201219217, arXiv: 1205.1688.

Beuermann, K., Euchner, F., Reinsch, K., Jordan, S., Gänsicke, B.T., 2007. Zeeman tomography of magnetic white dwarfs. IV. The complex field structure of the polars EF Eridani, BL Hydri and CP Tucanae. A&A 463, 647–655. https://doi.org/10.1051/0004-6361:20066332, arXiv: 0610804.

Bird, A.J., Bazzano, A., Malizia, A., Fiocchi, M., Sguera, V., Bassani, L., Hill, A.B., Ubertini, P., Winkler, C., 2016. The IBIS soft gamma-ray sky after 1000 integral orbits. ApJs 223, 15. https://doi.org/10.3847/0067-0049/223/1/15, arXiv: 1601.06074.

Brunschweiger, J., Greiner, J., Ajello, M., Osborne, J., 2009. Intermediate polars in the Swift/BAT survey: spectra and white dwarf masses. A&A 496, 121–127. https://doi.org/10.1051/0004-6361/200811285, arXiv: 0901.3562.

Buckley, D.A.H., Haberl, F., Motch, C., Pollard, K., Schwarzenberg-Czerny, A., Sekiguchi, K., 1997. ROSAT observations of RX J1712.6-2414: a discless intermediate polar?. MNRAS 287, 117–123. https://doi.org/10.1093/mnras/287.1.117.

Canalle, J.B.G., Saxton, C.J., Wu, K., Cropper, M., Ramsay, G., 2005. Accretion in dipole magnetic fields: flow structure and X-ray emission of accreting white dwarfs. A&A 440, 185–198. https://doi.org/10.1051/0004-6361:20052706, arXiv: 0504061.

Coti Zelati, F., Rea, N., Campana, S., de Martino, D., Papitto, A., Safi-Harb, S., Torres, D.F., 2016. Multiwavelength study of RX J2015.6+3711: a magnetic cataclysmic variable with a 2-h spin period. MNRAS 456, 1913–1923. https://doi.org/10.1093/mnras/stv2803, arXiv: 1510.04431.

Cropper, M., 1990. The Polars. SSRv 54, 195–295. https://doi.org/10.1007/BF00177799.

Cropper, M., Wu, K., Ramsay, G., Kocabiyik, A., 1999. Effects of gravity on the structure of post-shock accretion flows in magnetic cataclysmic variables. MNRAS 306, 684–690. https://doi.org/10.1046/j.1365-8711.1999.02570.x, arXiv: astro-ph/9902355.

Cusumano, G., Segreto, A., La Parola, V., Maselli, A., 2014. The 4th Palermo Swift-BAT catalogue: 100 months of survey of the hard X-ray sky. In: Proceedings of Swift: 10 Years of Discovery (SWIFT 10), held 2–5 December 2014 at La Sapienza University, Rome, Italy, p. 132.

de Martino, D., Belloni, T., Falanga, M., Papitto, A., Motta, S., Pellizzoni, A., Evangelista, Y., Piano, G., Masetti, N., Bonnet-Bidaud, J.-M., Mouchet, M., Mukai, K., Possenti, A., 2013. X-ray follow-ups of XSS J12270–4859: a low-mass X-ray binary with gamma-ray Fermi-LAT association. A&A 550, A89. https://doi.org/10.1051/0004-6361/201220393, arXiv: 1212.1615.

de Martino, D., Falanga, M., Bonnet-Bidaud, J.-M., Belloni, T., Mouchet, M., Masetti, N., Andruchow, I., Cellone, S., Mukai, K., Matt, G., 2010. The intriguing nature of the high-energy gamma ray source XSSJ12270-4859. A&A 515, A25. https://doi.org/10.1051/0004-6361/200913802, arXiv: 1002.3740.

de Martino, D., Matt, G., Belloni, T., Haberl, F., Mukai, K., 2004. BeppoSAX observations of soft X-ray intermediate polars. A&A 415, 1009–1019. https://doi.org/10.1051/0004-6361:20034160, arXiv: astro-ph/0311557.

de Martino, D., Matt, G., Mukai, K., Belloni, T., Bonnet-Bidaud, J.M., Chiappetti, L., Gänsicke, B.T., Haberl, F., Mouchet, M., 2001. The X-ray emission of the intermediate polar V 709 Cas. A&A 377, 499–511. https://doi.org/10.1051/0004-6361:20011059, arXiv: astro-ph/0107480.

de Martino, D., Matt, G., Mukai, K., Bonnet-Bidaud, J.-M., Falanga, M., Gänsicke, B.T., Haberl, F., Marsh, T.R., Mouchet, M., Littlefair, S.P., Dhillon, V., 2008. 1RXS J173021.5-055933: a cataclysmic variable with a fast-spinning magnetic white dwarf. A&A 481, 149–159. https://doi.org/10.1051/0004-6361:20078368, arXiv: 0801.3649.

de Martino, D., Matt, G., Mukai, K., Bonnet-Bidaud, J.-M., Gaensicke, B., Gonzalez-Perez, J., Haberl, F., Mouchet, M., Solheim, J.-E., 2005. X-ray confirmation of the intermediate polar HT Cam. A&A 437, 935–945. https://doi.org/10.1051/0004-6361:20052761, arXiv: astro-ph/0503470.

de Martino, D., Silvotti, R., Buckley, D.A.H., Gänsicke, B.T., Mouchet, M., Mukai, K., Rosen, S.R., 1999. Time-resolved HST and IUE UV spectroscopy of the intermediate polar FO AQR. A&A 350, 517–528, arXiv: astro-ph/9909069.

Done, C., Magdziarz, P., 1998. Complex absorption and reflection of a multitemperature cyclotron-bremsstrahlung X-ray cooling shock in BY Cam. MNRAS 298, 737–746. https://doi.org/10.1046/j.1365-8711.1998.01636.x, arXiv: astro-ph/9712226.

Echevarría, J., Ramírez-Torres, A., Michel, R., Hernández Santisteban, J. V., 2016. A radial velocity study of the intermediate polar EX Hydrae. MNRAS 461, 1576–1589. https://doi.org/10.1093/mnras/stw1425, arXiv: 1606.03734.

Esposito, P., Israel, G.L., de Martino, D., D'Avanzo, P., Testa, V., Sidoli, L., Di Stefano, R., Belfiore, A., Mapelli, M., Piranomonte, S., Rodríguez Castillo, G.A., Moretti, A., D'Elia, V., Verrecchia, F., Campana, S., Rea, N., 2015. Swift J201424.9+152930: discovery of a new deeply eclipsing binary with 491-s and 3.4-h modulations. MNRAS 450, 1705–1715. https://doi.org/10.1093/mnras/stv724, arXiv: 1503.08830.

Evans, P.A., Beardmore, A., Osborne, J., O'Brian, P., Willingale, R., Starling, R., Burrows, D.E.A., 2009. Methods and results of an automatic analysis of a complete sample of Swift-XRT observations of GRBs. MNRAS 397, 1177–1201. https://doi.org/10.1111/j.1365-2966.2009.14913.x, arXiv: 0812.3662.

Ezuka, H., Ishida, M., 1999. Iron line diagnostics of the Postshock hot plasma in magnetic cataclysmic variables observed with ASCA. ApJs 120, 277–298. https://doi.org/10.1086/313181.

Ferrario, L., de Martino, D., Gänsicke, B.T., 2015. Magnetic White Dwarfs. Space Sci. Rev. 191, 111–169. https://doi.org/10.1007/s11214-015-0152-0, arXiv: 1504.08072.

Fischer, A., Beuermann, K., 2001. Accretion physics of AM Herculis binaries. I. Results from one-dimensional stationary radiation hydrodynamics. A&A 373, 211–221. https://doi.org/10.1051/0004-6361:20010600, arXiv: 0105190.

Gabdeev, M.M., Shimanskiy, V.V., Borisov, N.V., Tazieva, Z.R., 2017. YY Sex: a Polar Candidate. In: Balega, Y.Y., Kudryavtsev, D.O., Romanyuk, I.I., Yakunin, I.A. (Eds.), Stars: From Collapse to Collapse. Astronomical Society of the Pacific Conference Series. vol. 510, pp. 435–438.

Garnavich, P., Szkody, P., 1988. Observed low states in DQ Herculis systems. PASP 100, 1522–1528. https://doi.org/10.1086/132358.

Goliasch, J., Nelson, L., 2015. Population synthesis of cataclysmic variables. I. Inclusion of detailed nuclear evolution. ApJ 809, 80. https://doi.org/10.1088/0004-637X/809/1/80, arXiv: 1607.06217.

Haberl, F., Motch, C., 1995. New intermediate polars discovered in the ROSAT survey: two spectrally distinct classes. A&A 297, L37–L40.

Haberl, F., Motch, C., Zickgraf, F.-J., 2002. X-ray and optical observations of 1RXS J154814.5-452845: a new intermediate polar with soft X-ray emission. A&A 387, 201–214. https://doi.org/10.1051/0004-6361:20020347, arXiv: astro-ph/0203227.

Hailey, C.J., Mori, K., Perez, K., Canipe, A.M., Hong, J., Tomsick, J.A., Boggs, S.E., Christensen, F.E., Craig, W.W., Fornasini, F., Grindlay, J.E., Harrison, F.A., Nynka, M., Rahoui, F., Stern, D., Zhang, S., Zhang, W.W., 2016. Evidence for intermediate Polars as the origin of the galactic center hard X-ray Emission. ApJ 826, 160. https://doi.org/10.3847/0004-637X/826/2/160, arXiv: 1605.06066.

Halpern, J.P., Thorstensen, J.R., Cho, P., Collver, G., Motsoaledi, M., Breytenbach, H., Buckley, D.A.H., Woudt, P.A., 2018. Optical studies

of 15 hard X-Ray selected cataclysmic binaries. AJ 155, 247. https://doi.org/10.3847/1538-3881/aabfd0, arXiv: 1804.08532.

Hameury, J.-M., Lasota, J.-P., 2017. The disappearance and reformation of the accretion disc during a low state of FO Aquarii. A&A 606, A7. https://doi.org/10.1051/0004-6361/201731226, arXiv: 1707.00540.

Hayashi, T., Ishida, M., 2014. A new comprehensive X-ray spectral model from the post-shock accretion column in intermediate polars. MNRAS 438, 2267–2277. https://doi.org/10.1093/mnras/stt2342.

Heard, V., Warwick, R.S., 2013. XMM-Newton observations of the Galactic Centre Region - I. The distribution of low-luminosity X-ray sources. MNRAS 428, 3462–3477. https://doi.org/10.1093/mnras/sts284, arXiv: 1210.6808.

Hellier, C., 1995. The accretion geometry of intermediate polars. In: Buckley, D.A.H.,Warner, B. (Eds.), Magnetic Cataclysmic Variables. Astronomical Society of the Pacific Conference Series. vol. 85, pp. 185–195.

Hellier, C., 2014. The Magnetospheric Boundary in Cataclysmic Variables. In: European Physical Journal Web of Conferences. European Physical Journal Web of Conferences. vol. 64, p. A07001. doi: https://doi.org/10.1051/epjconf/20136407001. arXiv:1312.4779.

Hong, J., Mori, K., Hailey, C.J., Nynka, M., Zhang, S., Gotthelf, E., Fornasini, F.M., Krivonos, R., Bauer, F., Perez, K., Tomsick, J.A., Bodaghee, A., Chiu, J.-L., Clavel, M., Stern, D., Grindlay, J.E., Alexander, D.M., Aramaki, T., Baganoff, F.K., Barret, D., Barrière, N., Boggs, S.E., Canipe, A.M., Christensen, F.E., Craig, W.W., Desai, M.A., Forster, K., Giommi, P., Grefenstette, B.W., Harrison, F.A., Hong, D., Hornstrup, A., Kitaguchi, T., Koglin, J.E., Madsen, K.K., Mao, P.H., Miyasaka, H., Perri, M., Pivovaroff, M.J., Puccetti, S., Rana, V., Westergaard, N.J., Zhang, W.W., Zoglauer, A., 2016. NuSTAR hard X-ray survey of the galactic center region. II. X-ray point sources. ApJ 825, 132. https://doi.org/10.3847/0004-637X/825/2/132, arXiv: 1605.03882.

Howell, S.B., Nelson, L.A., Rappaport, S., 2001. An exploration of the paradigm for the 2–3 hour period gap in cataclysmic variables. ApJ 550, 897–918. https://doi.org/10.1086/319776, arXiv: astro-ph/0005435.

in't Zand, J.J.M., Bozzo, E., Qu, J., Li, X.-D., Amati, L., Chen, Y., Donnarumma, I., Doroshenko, V., Drake, S.A., Hernanz, M., Jenke, P.A., Maccarone, T.J., Mahmoodifar, S., de Martino, D., De Rosa, A., Rossi, E.M., Rowlinson, A., Sala, G., Stratta, G., Tauris, T.M., Wilms, J., Wu, X., Zhou, P., Agudo, I., Altamirano, D., Atteia, J.-L., Andersson, N.A., Baglio, M.C., Ballantyne, D.R., Baykal, A., Behar, E., Belloni, T., Bhattacharyya, S., Bianchi, S., Bilous, A., Blay, P., Braga, J., Brandt, S., Brown, E.F., Bucciantini, N., Burderi, L., Cackett, E.M., Campana, R., Campana, S., Casella, P., Cavecchi, Y., Chambers, F., Chen, L., Chen, Y.-P., Chenevez, J., Chernyakova, M., Jin, C., Ciolfi, R., Costantini, E., Cumming, A., D'Aı', A., Dai, Z.-G., D'Ammando, F., De Pasquale, M., Degenaar, N., Del Santo, M., D'Elia, V., Di Salvo, T., Doyle, G., Falanga, M., Fan, X., Ferdman, R.D., Feroci, M., Fraschetti, F., Galloway, D.K., Gambino, A.F., Gandhi, P., Ge, M., Gendre, B., Gill, R., Götz, D., Gouiffès, C., Grandi, P., Granot, J., Güdel, M., Heger, A., Heinke, C.O., Homan, J., Iaria, R., Iwasawa, K., Izzo, L., Ji, L., Jonker, P.G., José, J., Kaastra, J.S., Kalemci, E., Kargaltsev, O., Kawai, N., Keek, L., Komossa, S., Kreykenbohm, I., Kuiper, L., Kunneriath, D., Li, G. et al., 2019. Observatory science with eXTP. Sci. China Phys. Mech. Astron. 62, 29506. doi:https://doi.org/10.1007/s11433-017-9186-1. arXiv:1812.04023.

Johnson, C.B., Torres, M.A.P., Hynes, R.I., Jonker, P.G., Heinke, C., Maccarone, T., Britt, C.T., Steeghs, D., Wevers, T., Wu, J., 2017. CXOGBS J174954.5-294335: a new deeply eclipsing intermediate polar. MNRAS 466, 129–137. https://doi.org/10.1093/mnras/stw3063, arXiv: 1612.01612.

Joshi, A., Pandey, J.C., Singh, K.P., Agrawal, P.C., 2016. PALOMA: a magnetic CV between Polars and intermediate Polars. ApJ 830, 56. https://doi.org/10.3847/0004-637X/830/2/56, arXiv: 1610.00557.

Kennedy, M.R., Callanan, P., Garnavich, P.M., Fausnaugh, M., Zinn, J. C., 2017a. XMM-Newton observations of the peculiar cataclysmic variable Lanning 386: X-ray evidence for a magnetic primary. MNRAS 466, 2202–2211. https://doi.org/10.1093/mnras/stw3282, arXiv: 1612.04397.

Kennedy, M.R., Garnavich, P.M., Littlefield, C., Callanan, P., Mukai, K., Aadland, E., Kotze, M.M., Kotze, E.J., 2017b. X-ray observations of FO Aqr during the 2016 low state. MNRAS 469, 956–967. https://doi.org/10.1093/mnras/stx880, arXiv: 1704.01909.

Knigge, C., Baraffe, I., Patterson, J., 2011. The evolution of cataclysmic variables as revealed by their donor stars. ApJs 194, 28. https://doi.org/10.1088/0067-0049/194/2/28, arXiv: 1102.2440.

Krivonos, R., Tsygankov, S., Lutovinov, A., Revnivtsev, M., Churazov, E., Sunyaev, R., 2012. INTEGRAL/IBIS nine-year Galactic hard X-ray survey. A&A 545, A27. https://doi.org/10.1051/0004-6361/201219617, arXiv: 1205.3941.

Littlefield, C., Garnavich, P., Kennedy, M.R., Patterson, J., Kemp, J., Stiller, R.A., Hambsch, F.-J., Arranz Heras, T., Myers, G., Stone, G., Sjoberg, G., Dvorak, S., Nelson, P., Popov, V., Bonnardeau, M., Vanmunster, T., de Miguel, E., Alton, K.B., Harris, B., Cook, L.M., Graham, K.A., Brincat, S.M., Lane, D.J., Foster, J., Pickard, R., Sabo, R., Vietje, B., Lemay, D., Briol, J., Krumm, N., Dadighat, M., Goff, W., Solomon, R., Padovan, S., Bolt, G., Kardasis, E., Debackere, A., Thrush, J., Stein, W., Coulter, D., Tsehmeystrenko, V., Gout, J.-F., Lewin, P., Galdies, C., Cejudo Fernandez, D., Walker, G., Boardman, J., Jr., & Pellett, E., 2019. The rise and fall of the king: the correlation between FO Aquarii's low states and the White Dwarf's Spindown. arXiv e-prints,. arXiv:1904.11505.

Littlefield, C., Stiller, R., Hambsch, F.-J., Shappee, B., Holoien, T., Garnavich, P., Kennedy, M., 2018. FO Aquarii begins its 2018 observing season with its third low state in two years. The Astronomer's Telegram, 11844.

Livio, M., Pringle, J.E., 1994. Star spots and the period gap in cataclysmic variables. ApJ 427, 956–960. https://doi.org/10.1086/174202.

Luna, G.J.M., Mukai, K., Orio, M., Zemko, P., 2018. Constraining the accretion geometry of the intermediate polar EX Hya using NuSTAR, Swift, and Chandra observations. ApJl 852, L8. https://doi.org/10.3847/2041-8213/aaa28f, arXiv: 1711.03942.

Lutovinov, A.A., Burenin, R.A., Revnivtsev, M.G., Suleimanov, V.F., Tkachenko, A.Y., 2010. IGR J16547–1916/1RXS J165443.5-191620:a new intermediate polar from the INTEGRAL galactic survey. Astron. Lett. 36, 904–909. https://doi.org/10.1134/S1063773710120042, arXiv: 1011.1129.

Masetti, N., Parisi, P., Jiménez-Bailón, E., Palazzi, E., Chavushyan, V., Bassani, L., Bazzano, A., Bird, A.J., Dean, A.J., Galaz, G., Landi, R., Malizia, A., Minniti, D., Morelli, L., Schiavone, F., Stephen, J.B., Ubertini, P., 2012. Unveiling the nature of INTEGRAL objects through optical spectroscopy. IX. Twenty two more identifications, and a glance into the far hard X-ray Universe. A&A 538, A123. https://doi.org/10.1051/0004-6361/201118559, arXiv: 1201.1906.

Masetti, N., Parisi, P., Palazzi, E., Jiménez-Bailón, E., Chavushyan, V., McBride, V., Rojas, A.F., Steward, L., Bassani, L., Bazzano, A., Bird, A.J., Charles, P.A., Galaz, G., Landi, R., Malizia, A., Mason, E., Minniti, D., Morelli, L., Schiavone, F., Stephen, J.B., Ubertini, P., 2013. Unveiling the nature of INTEGRAL objects through optical spectroscopy. X. A new multi-year, multi-observatory campaign. A&A 556, A120. https://doi.org/10.1051/0004-6361/201322026, arXiv: 1307.2898.

Masetti, N., Parisi, P., Palazzi, E., Jiménez-Bailón, E., Morelli, L., Chavushyan, V., Mason, E., McBride, V.A., Bassani, L., Bazzano, A., Bird, A.J., Dean, A.J., Galaz, G., Gehrels, N., Landi, R., Malizia, A., Minniti, D., Schiavone, F., Stephen, J.B., Ubertini, P., 2009. Unveiling the nature of INTEGRAL objects through optical spectroscopy. VII. Identification of 20 Galactic and extragalactic hard X-ray sources. A&A 495, 121–135. https://doi.org/10.1051/0004-6361:200811322, arXiv: 0811.4085.

Merloni, A., Predehl, P., Becker, W., Böhringer, H., Boller, T., Brunner, H., Brusa, M., Dennerl, K., Freyberg, M., Friedrich, P., Georgakakis, A., Haberl, F., Hasinger, G., Meidinger, N., Mohr, J., Nandra, K., Rau, A., Reiprich, T.H., Robrade, J., Salvato, M., Santangelo, A.,

Sasaki, M., Schwope, A., Wilms, J., & the German eROSITA Consortium, 2012. eROSITA Science Book: Mapping the Structure of the Energetic Universe. arXiv e-prints, arXiv:1209.3114.

Mukai, K., 2017. X-Ray emissions from accreting White Dwarfs: a review. PASP 129, 062001. https://doi.org/10.1088/1538-3873/aa6736, arXiv: 1703.06171.

Mukai, K., Ishida, M., Osborne, J., 1994. ASCA PV phase observations of FO Aqr. PASJ 46, L87–L91.

Mukai, K., Kallman, T., Schlegel, E., Bruch, A., Handler, G., Kemp, J., 2001. Chandra HETG observation of the magnetic cataclysmic variable V1223 Sagittarii. In: Inoue, H., Kunieda, H. (Eds.), New Century of X-ray Astronomy. Astronomical Society of the Pacific Conference Series. vol. 251, pp. 90–93.

Mukai, K., Rana, V., Bernardini, F., de Martino, D., 2015. Unambiguous detection of reflection in magnetic cataclysmic variables: joint NuSTAR-XMM-Newton observations of three intermediate polars. ApJl 807, L30. https://doi.org/10.1088/2041-8205/807/2/L30, arXiv: 1506.07213.

Muno, M.P., Baganoff, F.K., Bautz, M.W., Feigelson, E.D., Garmire, G. P., Morris, M.R., Park, S., Ricker, G.R., Townsley, L.K., 2004. Diffuse X-Ray emission in a deep Chandra image of the galactic center. ApJ 613, 326–342. https://doi.org/10.1086/422865, arXiv: astro-ph/0402087.

Nandra, K., Barret, D., Barcons, X., Fabian, A., den Herder, J.-W., Piro, L., Watson, M., Adami, C., Aird, J., Afonso, J.M., et al., 2013. The Hot and Energetic Universe: A White Paper presenting the science theme motivating the Athena+ mission. arXiv e-prints,. arXiv:1306.2307.

Nauenberg, M., 1972. Analytic approximations to the mass-radius relation and energy of zero-temperature stars. ApJ 175, 417–430.

Nobukawa, M., Uchiyama, H., Nobukawa, K.K., Yamauchi, S., Koyama, K., 2016. Origin of the galactic diffuse X-ray emission: iron k-shell line diagnostics. ApJ 833, 268. https://doi.org/10.3847/1538-4357/833/2/268, arXiv: 1701.00884.

Norton, A.J., Beardmore, A.P., Allan, A., Hellier, C., 1999. YY Draconis and V709 Cassiopeiae: two intermediate polars with weak magnetic fields. A&A 347, 203–211, arXiv: astro-ph/9811310.

Norton, A.J., Butters, O., Parker, T., Wynn, G.A., 2008. The accretion flows and evolution of MCVs. ApJ 672, 524–530. https://doi.org/10.1086/523932, arXiv: 0709.4186.

Norton, A.J., Hellier, C., Beardmore, A.P., Wheatley, P.J., Osborne, J.P., Taylor, P., 1997. Stream-fed and disc-fed accretion in TX Columbae. MNRAS 289, 362–370. https://doi.org/10.1093/mnras/289.2.362.

Norton, A.J., Watson, M.G., 1989. Spin modulated X-ray emission from intermediate polars. MNRAS 237, 853–874. https://doi.org/10.1093/mnras/237.4.853.

Norton, A.J., Wynn, G.A., Somerscales, R.V., 2004. The spin periods and magnetic moments of White Dwarfs in magnetic cataclysmic variables. ApJ 614, 349–357. https://doi.org/10.1086/423333, arXiv: astro-ph/0406363.

Norton, A.P., Beardmore, A.J., Taylor, P., 1996. On the interpretation of IP X-ray Power Spectra. MNRAS 280, 937–952. https://doi.org/10.1093/mnras/280.3.937.

Oh, K., Koss, M., Markwardt, C.B., Schawinski, K., Baumgartner, W.H., Barthelmy, S.D., Cenko, S.B., Gehrels, N., Mushotzky, R., Petulante, A., Ricci, C., Lien, A., Trakhtenbrot, B., 2018. The 105-month swift-BAT all-sky hard X-ray survey. ApJs 235, 4. https://doi.org/10.3847/1538-4365/aaa7fd, arXiv: 1801.01882.

Pagnotta, A., Schaefer, B.E., Clem, J.L., Landolt, A.U., Handler, G., Page, K.L., Osborne, J.P., Schlegel, E.M., Hoffman, D.I., Kiyota, S., Maehara, H., 2015. The 2010 Eruption of the Recurrent Nova U Scorpii: the multi-wavelength light curve. ApJ 811, 32. https://doi.org/10.1088/0004-637X/811/1/32, arXiv: 1509.05431.

Pala, A.F., Gänsicke, B.T., Townsley, D., Boyd, D., Cook, M.J., De Martino, D., Godon, P., Haislip, J.B., Henden, A.A., Hubeny, I., Ivarsen, K.M., Kafka, S., Knigge, C., LaCluyze, A.P., Long, K.S., Marsh, T.R., Monard, B., Moore, J.P., Myers, G., Nelson, P., Nogami, D., Oksanen, A., Pickard, R., Poyner, G., Reichart, D.E., Rodriguez Perez, D., Schreiber, M.R., Shears, J., Sion, E.M., Stubbings, R., Szkody, P., Zorotovic, M., 2017. Effective temperatures of cataclysmic-variable white dwarfs as a probe of their evolution. MNRAS 466, 2855–2878. https://doi.org/10.1093/mnras/stw3293, arXiv: 1701.02738.

Parisi, P., Masetti, N., Rojas, A.F., Jiménez-Bailón, E., Chavushyan, V., Palazzi, E., Bassani, L., Bazzano, A., Bird, A.J., Galaz, G., Minniti, D., Morelli, L., Ubertini, P., 2014. Accurate classification of 75 counterparts of objects detected in the 54-month Palermo Swift/BAT hard X-ray catalogue. A&A 561, A67. https://doi.org/10.1051/0004-6361/201322409, arXiv: 1311.1458.

Parker, T.L., Norton, A.J., Mukai, K., 2005. X-ray orbital modulations in intermediate polars. A&A 439, 213–225. https://doi.org/10.1051/0004-6361:20052887, arXiv: 0503658.

Perez, K., Hailey, C.J., Bauer, F.E., Krivonos, R.A., Mori, K., Baganoff, F.K., Barrière, N.M., Boggs, S.E., Christensen, F.E., Craig, W.W., Grefenstette, B.W., Grindlay, J.E., Harrison, F.A., Hong, J., Madsen, K.K., Nynka, M., Stern, D., Tomsick, J.A., Wik, D.R., Zhang, S., Zhang, W.W., Zoglauer, A., 2015. Extended hard-X-ray emission in the inner few parsecs of the Galaxy. Nature 520, 646–649. https://doi.org/10.1038/nature14353.

Potter, S.B., Buckley, D.A.H., 2018. Discovery of spin-modulated circular polarization from IGR J17014–4306, the remnant of Nova Scorpii 1437 AD. MNRAS 473, 4692–4697. https://doi.org/10.1093/mnras/stx2493, arXiv: 1709.08220.

Potter, S.B., Romero-Colmenero, E., Watson, C.A., Buckley, D.A.H., Phillips, A., 2004. Stokes imaging, Doppler mapping and Roche tomography of the AM Herculis system V834 Cen. MNRAS 348, 316–324. https://doi.org/10.1111/j.1365-2966.2004.07379.x, arXiv: astro-ph/0311151.

Pretorius, M.L., Knigge, C., Schwope, A.D., 2013. The space density of magnetic cataclysmic variables. MNRAS 432, 570–583. https://doi.org/10.1093/mnras/stt499, arXiv: 1303.4270.

Pretorius, M.L., Mukai, K., 2014. Constraints on the space density of intermediate polars from the Swift-BAT survey. MNRAS 442, 2580–2585. https://doi.org/10.1093/mnras/stu990, arXiv: 1405.3908.

Prialnik, D., Kovetz, A., 1995. An extended grid of multicycle nova evolution models. ApJ 445, 789–810. https://doi.org/10.1086/175741.

Ramsay, G., 2000. Determining the mass of the accreting white dwarf in magnetic cataclysmic variables using RXTE data. MNRAS 314, 403–408. https://doi.org/10.1046/j.1365-8711.2000.03239.x, arXiv: astro-ph/9912420.

Ramsay, G., Bridge, C., Cropper, M., Mason, K., Cordova, F., Priedhorsky, W., 2004. XMM-Newton observations of the eclipsing polar EP Dra. MNRAS 354, 773–778. https://doi.org/10.1111/j.1365-2966.2004.08239.x, arXiv: astro-ph/0407523.

Ramsay, G., Cropper, M., 2004. The energy balance of polars revisited. MNRAS 347, 497–507. https://doi.org/10.1111/j.1365-2966.2004.07220.x, arXiv: astro-ph/0309527.

Ramsay, G., Cropper, M., Mason, K.O., Córdova, F.A., Priedhorsky, W., 2004. XMM-Newton observations of three short-period polars: V347 Pav, GG Leo and EU UMa. MNRAS 347, 95–100. https://doi.org/10.1111/j.1365-2966.2004.07242.x, arXiv: astro-ph/0309110.

Ramsay, G., Cropper, M., Wu, K., Mason, K.O., Córdova, F.A., Priedhorsky, W., 2004. XMM-Newton observations of polars in low accretion states. MNRAS 350, 1373–1384. https://doi.org/10.1111/j.1365-2966.2004.07732.x, arXiv: astro-ph/0402526.

Ramsay, G., Rosen, S., Hakala, P., Barclay, T., 2009. 2XMMi J225036.9+573154 – a new eclipsing AM Her binary discovered using XMM-Newton. MNRAS 395, 416–421. https://doi.org/10.1111/j.1365-2966.2009.14528.x, arXiv: 0901.3095.

Rea, N., Zelati, F.C., Esposito, P., D'Avanzo, P., de Martino, D., Israel, G.L., Torres, D.F., Campana, S., Belloni, T.M., Papitto, A., Masetti, N., Carrasco, L., Possenti, A., Wieringa, M., Wilhelmi, E.D.O., Li, J., Bozzo, E., Ferrigno, C., Linares, M., Tauris, T.M., Hernanz, M., Ribas, I., Monelli, M., Borghese, A., Baglio, M.C., Casares, J., 2017. Multiband study of RX J0838–2827 and XMM J083850.4-282759: a new asynchronous magnetic cataclysmic variable and a candidate

transitional millisecond pulsar. MNRAS 471, 2902–2916. https://doi.org/10.1093/mnras/stx1560, arXiv: 1611.04194.

Reis, R., Wheatley, P., Gänsicke, B., Osborne, J., 2013. X-ray luminosities of optically selected cataclysmic variables and application to the Galactic ridge X-ray emission. MNRAS 430, 1994–2001. https://doi.org/10.1093/mnras/stt025, arXiv: 1301.1213.

Revnivtsev, M., Sazonov, S., Churazov, E., Forman, W., Vikhlinin, A., Sunyaev, R., 2009. Discrete sources as the origin of the Galactic X-ray ridge emission. Nature 458, 1142–1144. https://doi.org/10.1038/nature07946, arXiv: 0904.4649.

Revnivtsev, M., Sazonov, S., Gilfanov, M., Churazov, E., Sunyaev, R., 2006. Origin of the Galactic ridge X-ray emission. A&A 452, 169–178. https://doi.org/10.1051/0004-6361:20054268.

Ritter, H., Kolb, U., 2003. Catalogue of cataclysmic binaries, low-mass X-ray binaries and related objects (Seventh edition). A&A 404, 301–303. https://doi.org/10.1051/0004-6361:20030330, arXiv: astro-ph/0301444.

Rodríguez-Gil, P., Gänsicke, B.T., Hagen, H.-J., Araujo-Betancor, S., Aungwerojwit, A., Allende Prieto, C., Boyd, D., Casares, J., Engels, D., Giannakis, O., Harlaftis, E.T., Kube, J., Lehto, H., Martínez-Pais, I.G., Schwarz, R., Skidmore, W., Staude, A., Torres, M.A.P., 2007. SWSextantis stars: the dominant population of cataclysmic variables with orbital periods between 3 and 4h. MNRAS 377, 1747–1762. https://doi.org/10.1111/j.1365-2966.2007.11743.x, arXiv: 0704.1129.

Rosen, S.R., Mason, K.O., Cordova, F.A., 1988. EXOSAT X-ray observations of the eclipsing magnetic cataclysmic variable EX Hya. MNRAS 231, 549–573. https://doi.org/10.1093/mnras/231.3.549.

Saxton, C.J., Wu, K., Canalle, J.B.G., Cropper, M., Ramsay, G., 2007. X-ray emissions from two-temperature accretion flows within a dipole magnetic funnel. MNRAS 379, 779–790. https://doi.org/10.1111/j.1365-2966.2007.11958.x, arXiv: 0705.1331.

Schwope, A.D., 2018. Exploring the space density of X-ray selected cataclysmic variables. A&A 619, A62. https://doi.org/10.1051/0004-6361/201833723, arXiv: 1808.08144.

Schwope, A.D., Beuermann, K., Buckley, D.A.H., Ciardi, D., Cropper, M., Horne, K., Howell, S., Mantel, K.-H., Metzner, A., O'Brien, K., Schwarz, R., Sirk, M., Steeghs, D., Still, M., Thomas, H.-C., 1998. Polars - multisite emission – multiwavelength observation. In: Howell, S., Kuulkers, E., Woodward, C. (Eds.), Wild Stars in the Old West. Astronomical Society of the Pacific Conference Series. vol. 137, pp. 44–59. arXiv:astro-ph/9708228.

Schwope, A.D., Beuermann, K., Jordan, S., 1995. Magnetism in the polar BL Hydri. A&A 301, 447–455.

Schwope, A.D., Brunner, H., Buckley, D., Greiner, J., Heyden, K.V.D., Neizvestny, S., Potter, S., Schwarz, R., 2002. The census of cataclysmic variables in the ROSAT Bright Survey. A&A 396, 895–910. https://doi.org/10.1051/0004-6361:20021386, arXiv: astro-ph/0210059.

Shara, M.M., Iłkiewicz, K., Mikołajewska, J., Pagnotta, A., Bode, M.F., Crause, L.A., Drozd, K., Faherty, J., Fuentes-Morales, I., Grindlay, J. E., Moffat, A.F.J., Pretorius, M.L., Schmidtobreick, L., Stephenson, F.R., Tappert, C., Zurek, D., 2017. Proper-motion age dating of the progeny of Nova Scorpii AD 1437. Nature 548, 558–560. https://doi.org/10.1038/nature23644, arXiv: 1704.00086.

Shara, M.M., Yaron, O., Prialnik, D., Kovetz, A., 2010. Non-equipartition of Energy, Masses of Nova Ejecta, and Type Ia Supernovae. ApJl 712, L143–L147. https://doi.org/10.1088/2041-8205/712/2/L143, arXiv: 1002.2303.

Shaw, A.W., Heinke, C.O., Mukai, K., Sivakoff, G.R., Tomsick, J.A., Rana, V., 2018. Measuring the masses of intermediate polars with NuSTAR: V709 Cas, NY Lup, and V1223 Sgr. MNRAS 476, 554–561. https://doi.org/10.1093/mnras/sty246, arXiv: 1801.08508.

Starrfield, S., Iliadis, C., Hix, W.R., Timmes, F.X., Sparks, W.M., 2009. The effects of the pep nuclear reaction and other improvements in the nuclear reaction rate library on simulations of the Classical Nova Outburst. ApJ 692, 1532–1542. https://doi.org/10.1088/0004-637X/692/2/1532, arXiv: 0811.0197.

Staude, A., Schwope, A.D., Schwarz, R., Vogel, J., Krumpe, M., Nebot Gomez-Moran, A., 2008. The changing accretion states of the intermediate polar MU Camelopardalis. A&A 486, 899–909. https://doi.org/10.1051/0004-6361:20067013, arXiv: 0806.0793.

Suleimanov, V., Doroshenko, V., Ducci, L., Zhukov, G.V., Werner, K., 2016. GK Persei and EX Hydrae: intermediate polars with small magnetospheres. A&A 591, A35. https://doi.org/10.1051/0004-6361/201628301, arXiv: 1604.00232.

Suleimanov, V., Poutanen, J., Falanga, M., Werner, K., 2008. Influence of Compton scattering on the broad-band X-ray spectra of intermediate polars. A&A 491, 525–529. https://doi.org/10.1051/0004-6361:200810119, arXiv: 0805.0427.

Suleimanov, V., Revnivtsev, M., Ritter, H., 2005. RXTE broad band X-ray spectra of IPs and WD masses. A&A 435, 191–199. https://doi.org/10.1051/0004-6361:20041283, arXiv: astro-ph/0405236.

Suleimanov, V.F., Doroshenko, V., Werner, K., 2019. Hard X-ray view on intermediate polars in the Gaia era. MNRAS 482, 3622–3635. https://doi.org/10.1093/mnras/sty2952, arXiv: 1809.05740.

Szkody, P., Nishikida, K., Erb, D., Mukai, K., Hellier, C., Uemura, M., Kato, T., Pavlenko, E., Katysheva, N., Shugarov, S., Cook, L., 2002. X-ray/optical studies of two outbursts of the intermediate polar YY (DO) Draconis. AJ 123, 413–419. https://doi.org/10.1086/324733.

Thorstensen, J.R., Halpern, J., 2013. Optical and X-ray studies of 10 X-ray-selected cataclysmic binaries. AJ 146, 107. https://doi.org/10.1088/0004-6256/146/5/107, arXiv: 1308.5016.

Thorstensen, J.R., Taylor, C.J., Peters, C.S., Skinner, J.N., Southworth, J., Gänsicke, B.T., 2015. Spectroscopic orbital periods for 29 cataclysmic variables from the Sloan Digital Sky Survey. AJ 149, 128. https://doi.org/10.1088/0004-6256/149/4/128, arXiv: 1502.02085.

Tomsick, J.A., Rahoui, F., Krivonos, R., Clavel, M., Strader, J., Chomiuk, L., 2016. Identifying IGR J14091–6108 as a magnetic CV with a massive white dwarf using X-ray and optical observations. MNRAS 460, 513–523. https://doi.org/10.1093/mnras/stw871, arXiv: 1604.03562.

Tout, C.A., Wickramasinghe, D.T., Liebert, J., Ferrario, L., Pringle, J.E., 2008. Binary star origin of high field magnetic white dwarfs. MNRAS 387, 897–901. https://doi.org/10.1111/j.1365-2966.2008.13291.x, arXiv: 0805.0115.

Tovmassian, G., González-Buitrago, D., Thorstensen, J., Kotze, E., Breytenbach, H., Schwope, A., Bernardini, F., Zharikov, S.V., Hernandez, M.S., Buckley, D.A.H., de Miguel, E., Hambsch, F.-J., Myers, G., Goff, W., Cejudo, D., Starkey, D., Campbell, T., Ulowetz, J., Stein, W., Nelson, P., Reichart, D.E., Haislip, J.B., Ivarsen, K.M., LaCluyze, A.P., Moore, J.P., Miroshnichenko, A.S., 2017. IGR J19552+0044: a new asynchronous short period polar. Filling the gap between intermediate and ordinary polars. A&A 608, A36. https://doi.org/10.1051/0004-6361/201731323, arXiv: 1710.02126.

van Teeseling, A., Heise, J., Paerels, F., 1994. X-ray irradiation of white dwarf atmospheres: the soft X-ray spectrum of AM Herculis. A&A 281, 119–128.

Wada, Y., Yuasa, T., Nakazawa, K., Makishima, K., Hayashi, T., Ishida, M., 2018. An estimation of the white dwarf mass in the Dwarf Nova GK Persei with NuSTAR observations of two states. MNRAS 474, 1564–1571. https://doi.org/10.1093/mnras/stx2880, arXiv: 1711.01727.

Warner, B., 1995. Cataclysmic variable stars. Cambridge University Press, Cambridge.

Warwick, R.S., Byckling, K., Pérez-Ramírez, D., 2014. The Galactic plane at faint X-ray fluxes - II. Stacked X-ray spectra of a sample of serendipitous XMM-Newton sources. MNRAS 438, 2967–2979. https://doi.org/10.1093/mnras/stt2413, arXiv: 1401.3116.

Wickramasinghe, D.T., Ferrario, L., 2000. Magnetism in isolated and binary White Dwarfs. PASP 112, 873–924. https://doi.org/10.1086/316593.

Wickramasinghe, D.T., Tout, C.A., Ferrario, L., 2014. The most magnetic stars. MNRAS 437, 675–681. https://doi.org/10.1093/mnras/stt1910, arXiv: 1310.2696.

Wickramasinghe, D.T., Wu, K., 1994. A new evolutionary model for Am-Herculis binaries. MNRAS 266, L1–L4. https://doi.org/10.1093/mnras/266.1.L1.

Woelk, U., Beuermann, K., 1992. Particle heated atmospheres of magnetic white dwarfs. A&A 256, 498–506.

Woelk, U., Beuermann, K., 1996. Stationary radiation hydrodynamics of accreting magnetic white dwarfs. A&A 306, 232–240.

Worpel, H., Schwope, A.D., Granzer, T., Reinsch, K., Schwarz, R., Traulsen, I., 2016. X-ray and optical observations of four polars. A&A 592, A114. https://doi.org/10.1051/0004-6361/201628650, arXiv: 1605.00927.

Wu, K., Chanmugam, G., Shaviv, G., 1994. Structure of steady state accretion shocks with several cooling functions: Closed integral-form solution. ApJ 426, 664–668. https://doi.org/10.1086/174103.

Wynn, G.A., King, A.R., 1992. Theoretical X-ray power spectra of intermediate polars. MNRAS 255, 83–91. https://doi.org/10.1093/mnras/255.1.83.

Xu, X.-J., Wang, Q.D., Li, X.-D., 2016. Fe line diagnostics of cataclysmic variables and galactic ridge X-ray emission. ApJ 818, 136. https://doi.org/10.3847/0004-637X/818/2/136, arXiv: 1602.05262.

Yaron, O., Prialnik, D., Shara, M.M., Kovetz, A., 2005. An extended grid of nova models. II. The parameter space of Nova Outbursts. ApJ 623, 398–410. https://doi.org/10.1086/428435, arXiv: astro-ph/0503143.

Zorotovic, M., Schreiber, M.R., Gänsicke, B.T., 2011. Post common envelope binaries from SDSS. XI. The white dwarf mass distributions of CVs and pre-CVs. A&A 536, A42. https://doi.org/10.1051/0004-6361/201116626, arXiv: 1108.4600.

Please cite this article as: D. de Martino, F. Bernardini, K. Mukai et al., Hard X-ray cataclysmic variables, Advances in Space Research, https://doi.org/10.1016/j.asr.2019.09.006